

MODELLING AND SIMULATION OF DOUBLY-FED INDUCTION GENERATOR CONNECTED WITH WIND TURBINE

By

NITEESH SONKER (111EE0054)

SOUMYA RANJAN DAS (111EE0207)

LAXMAN MOHAPATRO (111EE0220)



**DEPARTMENT OF ELECTRICAL ENGINEERING
NATIONAL INSTITUTE OF TECHNOLOGY
ROURKELA, ODISHA**

MODELLING AND SIMULATION OF DOUBLY-FED INDUCTION GENERATOR CONNECTED WITH WIND TURBINE

*A Thesis submitted in partial fulfilment of the requirements for the degree of
Bachelor of Technology in “Electrical Engineering”*

By

**NITEESH SONKER (111EE0054)
SOUMYA RANAJN DAS (111EE0207)
LAXMAN MOHAPATRO (111EE0220)**

**Under guidance of
Dr. Sanjib Ganguly**



**DEPARTMENT OF ELECTRICAL ENGINEERING
NATIONAL INSTITUTE OF TECHNOLOGY
ROURKELA, ODISHA**

ACKNOWLEDGEMENT

We have been extremely lucky to have Dr. Sanjib Ganguly, Department of Electrical Engineering, NIT, Rourkela as our Project Guide. He enlivened us to make enthusiasm for Wind Energy Systems, taught us nature and standard of exploration and guided us through the culmination of this postulation work. Working with Dr. Sanjib Ganguly was very delightful, rousing and learning background. We are obliged to him and express our profound feeling of appreciation for his direction and backing. We are exceedingly obliged for the support of Department of Electrical Engineering, NIT, Rourkela for giving us different offices which have been exceptionally valuable.

We express uncommon because of every one of our companions, for being there, at whatever point we required them. We devote this Thesis to my family and companions.

NITEESH SONKER (111EE0054)

SOUMYA RANJAN DAS (111EE0207)

LAXMAN MOHAPATRO (111EE0220)

B.TECH, ELECTRICAL ENGINEERING
NIT, Rourkela



**DEPARTMENT OF ELECTRICAL ENGINEERING
NATIONAL INSTITUTE OF TECHNOLOGY
ROURKELA, ODISHA**

CERTIFICATE

This is to confirm that the thesis entitled "Modelling and Simulation of Doubly Fed Induction Generator Based Wind Turbine", submitted by Niteesh Sonker (111EE0054), Soumya Ranjan Das(111EE0207) and Laxman Mohapatro (110EE0220) in partial satisfaction of the necessities for the grant of Bachelor of Technology in Electrical Engineering amid session 2014-2015 at National Institute of Technology, Rourkela. A bonafide record of project work has been done by them under my guidance and supervision.

The students have satisfied all the recommended prerequisites. The Thesis which is in view of students own work, have not submitted somewhere else for a Degree/ Diploma. In my view, the thesis is of standard needed for the recompense of a Bachelor of Technology degree in Electrical Engineering.

**Place: Rourkela
Dept. of Electrical Engineering
National institute of Technology
Rourkela-769008**

**Dr. Sanjib Ganguly
Assistant Professor**

ABSTRACT

This work presents the modelling of DFIG (Doubly-Fed Induction Machine) using active and reactive power transfer model and the controlling strategy of DFIG using multivariable control method. This paper also represents the free acceleration characteristics of the machine. Real/Reactive powers are used in the matrix as state variables. Multi-loop control scheme is used for the control. The controller part uses six compensators. The matrix method used this paper increased the robustness of the machine as power waveforms are independent of d-q reference variable. The simulation of modelling and controlling is done using MATLAB/SIMULINK and the waveforms are plotted.

CONTENTS

Acknowledgement	3
Certificate	4
Abstract	5
Symbols Used	8
Figures List	9-10
Chapter-1 : Introduction	
1.1 Wind Energy	11
1.2 Terms And Definitions	11
1.2.1 Power Contained in the Wind	11
1.2.2 Tip speed Ratio	11
1.2.3 Power coefficient	12
1.2.4 Pitch Angle	12
1.3 Types of Wind Turbine	12
1.3.1 Constant-Speed Wind Turbine	12
1.3.2 Variable Speed Wind Turbine	13
1.3.3 Variable Speed Wind Turbine with DFIG	13
1.3.4 DFIG Systems for Wind Turbines	14
1.4 Power Flow in DFIG	14-15
Chapter-2: Modelling of Doubly-Fed Induction Generator	
2.1 Transformation of abc to dq0 reference	16-18
2.2 Modelling of DFIG Wind Energy Systems	18-20
2.3 Modelling of DFIG Using Instantaneous Power Components	20-23
2.4 Grid-Side Converter and Filter Model	23-25
2.5 Model OF Wind Turbine	25
2.6 Linearization of model of a DFIG machine	26-28

2.7 Free acceleration characteristics of induction machine	28
Chapter-3: Control Strategy of DFIG	
3.1 Sequential loop closing	29
3.2 Design of control system for a DFIG wind turbine system	
3.2.1 Controller Design Method	29
3.2.2 Design of the Rotor-Side Controllers	30-31
3.2.3 Rotor Speed Controller Design	31
3.2.4 Grid-Side Controller Design	31-32
3.2.5 DC-Link Voltage Controller Design	32-33
3.3 Parameters calculation for controllers	33-34
Chapter-4: Simulation and Results	
4.1 Design of Wind Turbine	35-36
4.2 Torque-Slip characteristics of Induction machine	36
4.3 Simulink for controlling of DFIG	37-40
4.4 Free acceleration characteristics of Induction Machine	41-45
Conclusion	46
References	47-48
Appendix	49

NOTATION AND SYMBOL USED

L_s = stator inductance

L_m = magnetizing inductance

L_r = rotor inductances

ω_r = rotor speed of the induction machine

ω_{sl} = slip frequency

$p_g(t)$ = instantaneous grid side active power

$q_g(t)$ = instantaneous grid side reactive power

$p_r(t)$ = instantaneous rotor side active power

$q_r(t)$ = instantaneous rotor side reactive power

V_{dc} = DC link voltage

v_{sdq} = stator dq reference voltage

v_{rdq} = rotor dq reference voltage

i_{sdq} = stator dq reference current

i_{rdq} = rotor dq reference current

ψ_{sdq} = stator flux in dq frame

ψ_{rdq} = rotor flux in dq frame

u_{rd}, u_{rd} = variables containing rotor side dq voltage

u_{gd}, u_{gd} = variables containing grid side dq voltage

P_m = mechanical input power

T_m = mechanical torque

T_e = electromagnetic torque

P = number of poles

J = moment of inertia of wind turbine ($\text{Kg} \cdot \text{m}^2$)

LIST OF FIGURES

Fig 1.1 - Schematic Diagram for Fixed speed Wind Turbine

Fig 1.2 - Schematic Diagram for Variable speed Wind Turbine

Fig 1.3- Schematic diagram for Doubly-fed Wind Turbine

Fig 1.4 Doubly-Fed Induction Generator Principle

Fig 1.5- Flow of power in DFIG during Super-synchronous speed

Fig 1.6- Flow of power in DFIG during Sub-Synchronous mode

Fig 2.1 abc to dq0 reference axis

Fig.2.2 Schematic diagram of the DFIG based wind turbine system

Fig 2.3 Equivalent circuit of grid side filter

Fig.3.1 schematic diagram for the control of grid side and rotor side converters.

Fig.4.1(a) Power coefficient Vs Tip speed ratio characteristics

Fig 4.1(b)- Power output of turbine Vs Wind speed characteristics

Fig 4.2- Torque vs speed characteristics

Fig.4.3 Simulink Block Diagram for controlling of DFIG

Fig.4.3.1 wind speed variation with time

Fig 4.3.2 Three phase supply to stator

Fig 4.3.3 Stator voltage along d-axis

Fig 4.3.4 Stator voltage along q-axis

Fig 4.3.5 Stator active power

Fig 4.3.6 Grid-side active power

Fig 4.3.7 Rotor reactive power

Fig 4.3.8 grid reactive power

Fig 4.3.9 stator reactive power

Fig 4.4.1- Simulink Block Diagram for Free acceleration characteristics of Induction machine

Fig 4.4.2 Simulink Block Diagram for Modelling of DFIG

Fig 4.4.3 Torque-speed characteristics

Fig 4.4.4 Stator a-phase current

Fig 4.4.5 Stator b-phase current

Fig 4.4.6 stator c-phase current

Fig 4.4.7 Rotor a-phase current

Fig 4.4.8 Rotor b-phase current

Fig 4.4.9 Rotor c-phase current

Fig 4.4.10 Electromagnetic torque during free acceleration

Fig 4.4.11 Rotor speed variation during free acceleration mode

CHAPTER-1

INTRODUCTION

1.1 Motivation

Energy of wind is the most accessible and exploitable types of renewable vitality. Because of rapidly need for electrical energy and exhaustion of fossil fuels, for example, coal and oil, whose stores are restricted, this issues drove researchers to create another source of energy for era of power. The most reluctant source which fulfills non-contamination, accessible in wealth, less costlier to tackle both in low-scale and high-scale frameworks is wind.

For variable speed range, power can be supplied to grid by controlling rotor power from a variable frequency source for slip-ring induction machine. The bidirectional flow of power from rotor of the induction machine can be done by connecting ac/dc/ac converters across the rotor. This type of system is called Doubly-Fed Induction Generator (DFIG) where power flows bi-directionally.

1.2 Terms and Definitions -

1.2.1 Power contained in the wind-

The kinetic energy of the air masses per unit time.[1]

$$P_0 = \frac{1}{2} \times (\text{Air mass per unit time}) \times (\text{wind velocity})^2$$

$$P_0 = \frac{1}{2} \rho A V_w^3 \quad (1.1)$$

1.2.2 Tip speed Ratio (TSR)-

The ratio of the wind flowing from the tip of the blade to the wind velocity. It is denoted by λ . [1]

$$\lambda = \frac{2\pi RN}{V_w} \quad (1.1)$$

1.2.3 Power coefficient-

The ratio of power output of the machine to the power contained in the wind. It is denoted by C_p . [1]

1.2.4 Pitch Angle-

It is angle between the chord of aerofoil section and the plane of revolution..

1.3 Types of Wind Turbine System -

1.3.1 Constant - Speed Wind Turbine System-

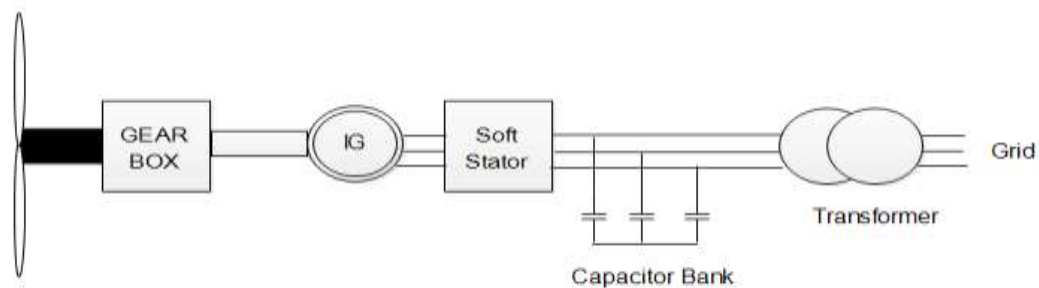


Fig 1.1 - Schematic Diagram for Fixed speed Wind Turbine

1.3.2 Variable-Speed Wind Turbine System-

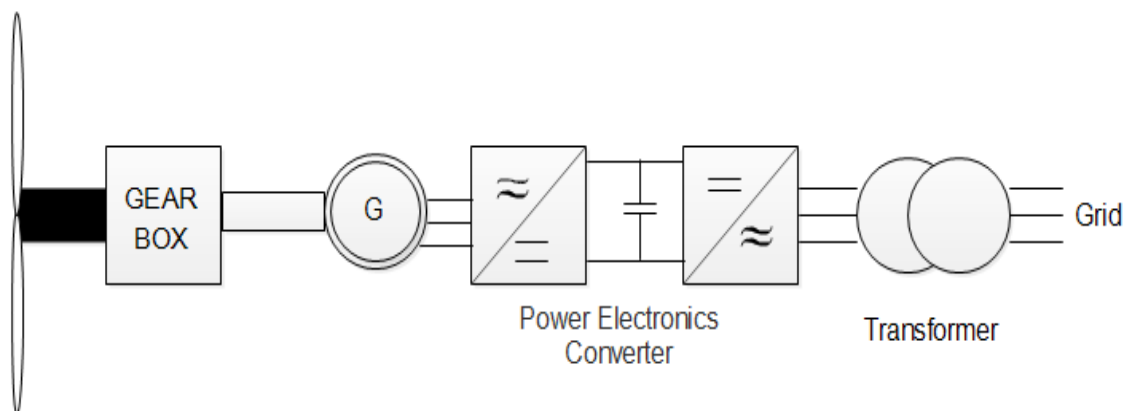


Fig 1.2 - Schematic Diagram for Variable-speed Wind Turbine

1.3.3 Variable-Speed Wind Turbine with Doubly-Fed Induction Generator-

The diagram, as indicated in Fig.1.3 involves a DFIG wind turbine. In this scheme the stator is directly connected to the grid and the rotor is connected to the grid through a converter. This scheme requires converter of lesser rating since the converter handles 20%-30% of total power. So power losses in the converter will be less, comparing to other various types of wind system. So cost of converter is less. Grid side converter is used to maintain dc-link voltage constant and rotor side converter is used to control power flow through rotor at different rotor speed. [1]

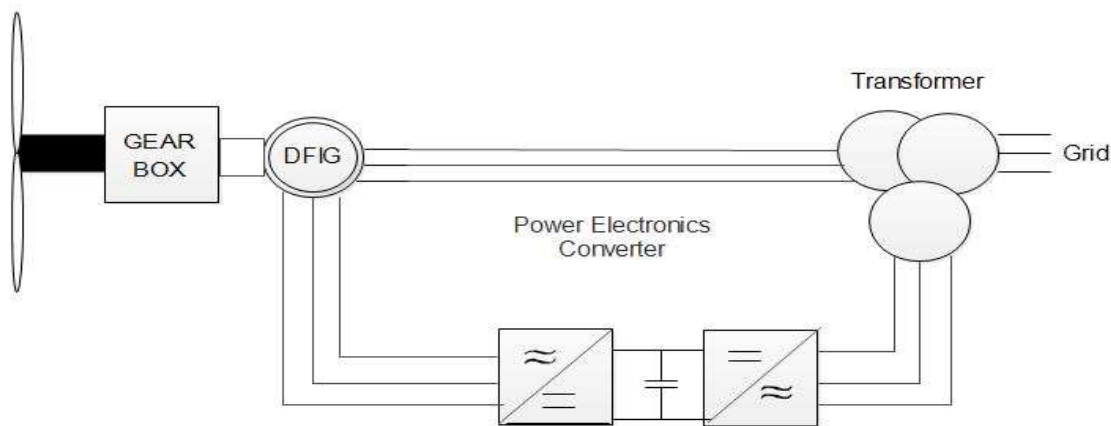


Fig 1.3- Schematic diagram for Doubly-fed Wind Turbine

1.3.4 Doubly-Fed Induction Generator Systems for Wind Turbines

The scheme shown below is used for variable speed operation about thirty percent of synchronous speed. 20-30% of the total power flowing through grid or vice versa is controlled by power electronic converter. The power factor of the overall system will be one.

The converter are controlled by PWM Pulse generators.

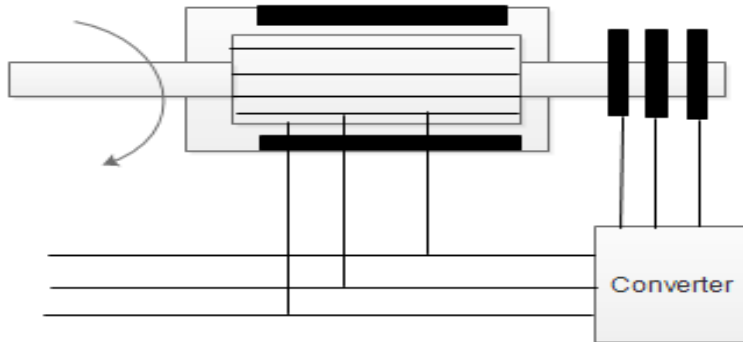


Fig 1.4 Doubly-Fed Induction Generator Principle

The converters are connected in back to back fashion with a transformer to the grid that includes two converters. In between the two converters a dc capacitor is connected, to keep the voltage variances (or swell) in the link voltage to a minimum quantity.

1.4 Power flow in DFIG

To compute the power flow of the DFIG scheme, the apparent power is fed to the DFIG through the stator and rotor circuit must be resolved. DFIG can run in two method for operation, for example, sub-synchronous and super-synchronous mode in view of the rotor speed beneath or more the synchronous speed. The flow of power in the rotor of a doubly fed induction machine has three parts.[1,2]

These are

- 1) The electromagnetic power traded between the stator and the rotor through the air gap which can be characterized as the air gap power P_s .
- 2) The mechanical force P_m traded between the rotor and shaft.
- 3) P_r (slip power) which is exchanged between the rotor and load through the rotor slip-rings. These three segments of rotor force are subordinate, in sub- and super-synchronous methods of operation, as indicated in figure 1.5

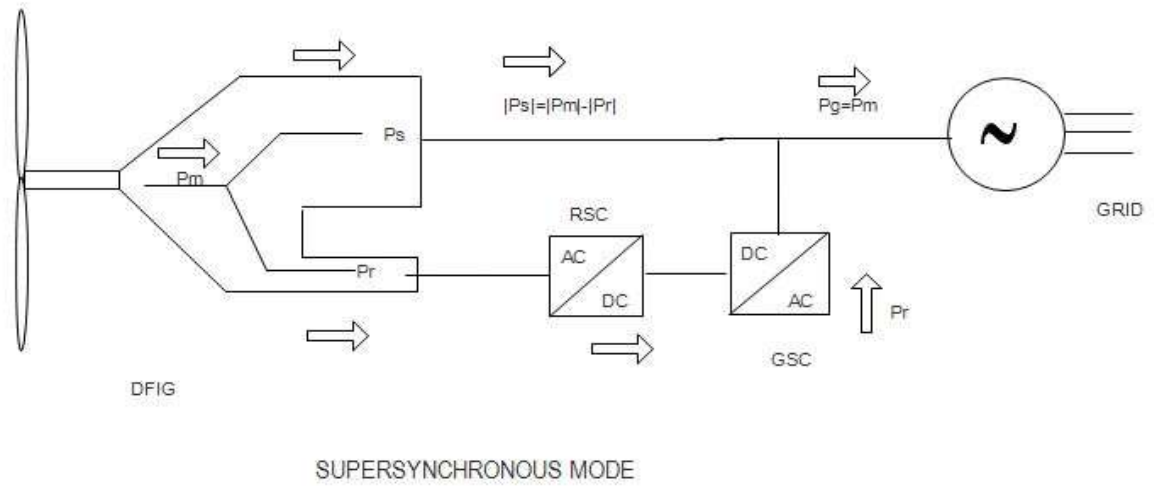


Fig 1.5- Power flow in DFIG during Super-synchronous speed

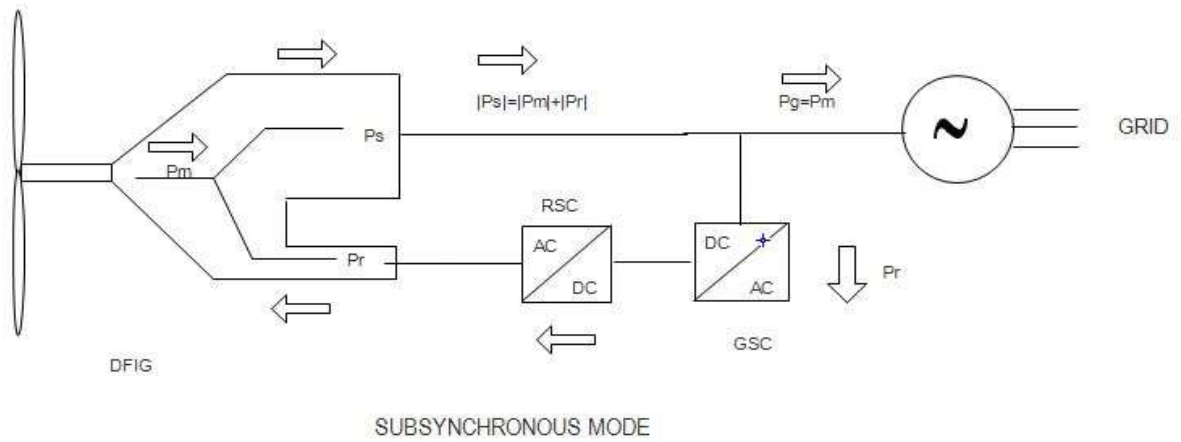


Fig 1.6- Power flow in DFIG during Sub-Synchronous speed

CHAPTER-2

MODELLING OF DOUBLY-FED INDUCTION GENERATOR (DFIG)

2.1 Transformation of abc to dq0 reference-

Changes of variables are utilized for the analysis of ac machines to remove time-differing inductances, changes of variables are additionally utilized in the analysis of different static, consistent parameter power-system segments connected with electric drives.

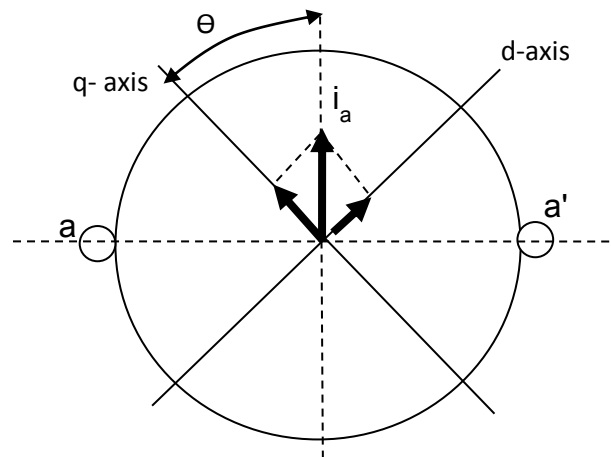


Fig 2.1 abc to dq0 reference axis

The foundation of the vector control procedure is d-q axis theory and its study is vital for vector control analysis.

dq0 or direct-quadrature-zero change is utilized to improve the analysis of three phase circuits, here three AC quantities are changed into two DC quantities which are done in light of the imaginary DC quantities and the AC quantities are again recovered by taking an reverse change of the DC quantities. It tackles the issue of AC parameters changing with time.

.The orthogonally placed balanced windings, are known as d- and q- windings which are dealt with as stationary or moving in respect to the stator.

In the stationary edge of reference, the d-q axis are viewed as fixed on the stator, with either d or q axis corresponding with the a-phases axis of the stator. In the rotating frame, the rotating d-q axis are considered either fixed on the rotor or made to move at the synchronous speed.

Park's transformation considers a frame of reference on the rotor. The scientist Parks gave this for a synchronous machine which is the same as a synchronous frame of reference. For induction motors, it is necessary to distinguish between a synchronous reference frame and a reference frame on the rotor.

In fig. the projection of the a-b-c currents as having sinusoidal variation in time along their respective axes (a space vector!), is seen. The picture illustrates for the a-phase. Similarly, b-phase currents and the c-phase currents are decomposed along dq-axis, and on adding them up, it gives:

$$i_d = k_d(i_a \sin(\theta) + i_b \sin(\theta - 120^\circ) + i_c \sin(\theta + 120^\circ)) \quad (2.1)$$

$$i_q = k_q(i_a \cos(\theta) + i_b \cos(\theta - 120^\circ) + i_c \cos(\theta + 120^\circ)) \quad (2.2)$$

Here k_q and k_d are constants.

As here 3 variables i_a , i_b , and i_c are transformed into two variables i_d and i_q , this gives an undetermined system. i.e. the transformation i_a , i_b , and i_c to i_d and i_q is unique while transformation i_d and i_q to i_a , i_b , and i_c is not unique. Hence we need a third current the zero-sequence current which is given as:

$$i_0 = k_0(i_a + i_b + i_c) \quad (2.3)$$

In matrix form these equations can be written as:

$$\begin{bmatrix} i_q \\ i_d \\ i_0 \end{bmatrix} = \begin{bmatrix} k_q \cos(\theta) & k_q \cos(\theta - 120^\circ) & k_q \cos(\theta + 120^\circ) \\ k_d \sin(\theta) & k_d \sin(\theta - 120^\circ) & k_d \sin(\theta + 120^\circ) \\ k_0 & k_0 & k_0 \end{bmatrix} \begin{bmatrix} i_a \\ i_b \\ i_c \end{bmatrix} \quad (2.4)$$

The constants k_0 , k_q , and k_d are selected as $1/3$, $2/3$, and $2/3$, respectively, which results the magnitude of the d-q quantities to be equal to that of the three-phase quantities. Some author uses its different values such as according to Anderson & Fouad use $k_0=1/\sqrt{3}$, $k_d=k_q=\sqrt{2/3}$.

Finally the abc to dq0 transformation is expressed as :

$$\begin{bmatrix} i_q \\ i_d \\ i_0 \end{bmatrix} = \frac{2}{3} \begin{bmatrix} \cos(\theta) & \cos(\theta - 120^\circ) & \cos(\theta + 120^\circ) \\ \sin(\theta) & \sin(\theta - 120^\circ) & \sin(\theta + 120^\circ) \\ 0.5 & 0.5 & 0.5 \end{bmatrix} \begin{bmatrix} i_a \\ i_b \\ i_c \end{bmatrix} \quad (2.5)$$

$$f_{dq0} = T f_{abc} \quad (2.6)$$

Where

$$T = \frac{2}{3} \begin{bmatrix} \cos(\theta) & \cos(\theta - 120^\circ) & \cos(\theta + 120^\circ) \\ \sin(\theta) & \sin(\theta - 120^\circ) & \sin(\theta + 120^\circ) \\ 0.5 & 0.5 & 0.5 \end{bmatrix} \quad (2.7)$$

Thus the dq0 to abc transformation is expressed as :

$$f_{abc} = T^{-1} f_{dq0} \quad (2.8)$$

Where

$$T^{-1} = \begin{bmatrix} \cos(\theta) & \sin(\theta) & 1 \\ \cos(\theta - 120^\circ) & \sin(\theta - 120^\circ) & 1 \\ \cos(\theta + 120^\circ) & \sin(\theta + 120^\circ) & 1 \end{bmatrix}$$

2.2 Modelling of DFIG Wind Energy Systems-

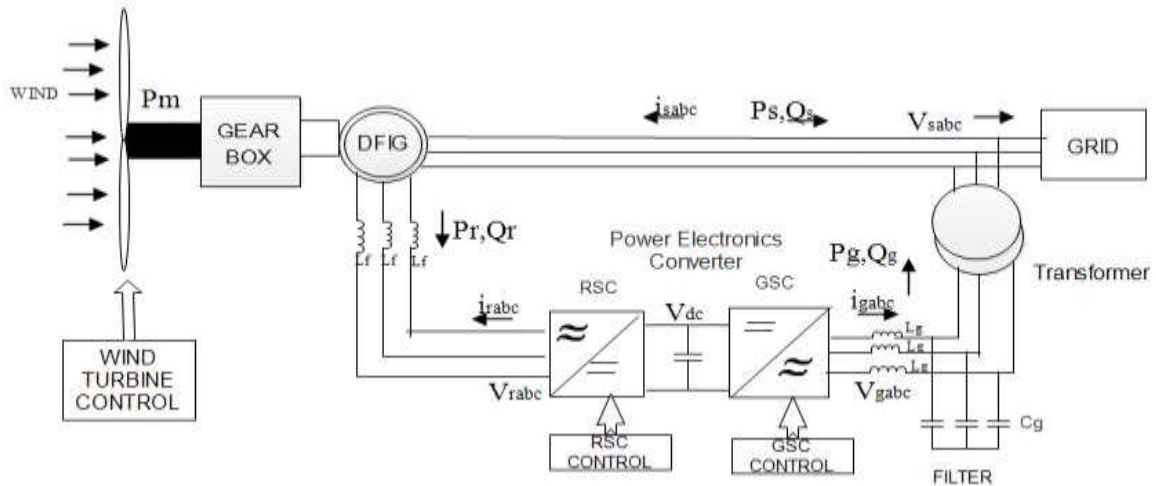


Fig.2.2 Schematic diagram of the DFIG-based wind generation system

Converter employs a rotor-side converter (RSC) and a Grid side converter (GSC) . Rotor-side converter (RSC) changes the speed of induction generator and a Grid side converter (GSC) injects reactive power to system via converter ,using passive sign convention instantaneous active and reactive power of the grid side converter are $p_g(t)$ and $q_g(t)$, and it is given as:[3]

$$\begin{bmatrix} p_g(t) \\ q_g(t) \end{bmatrix} = \frac{3}{2} \begin{bmatrix} v_{sd} & v_{sq} \\ v_{sq} & -v_{sd} \end{bmatrix} \begin{bmatrix} i_{gd} \\ i_{gq} \end{bmatrix} \quad (2.9)$$

Where, $v_{sd,sq}$ = dq component of stator voltage in the synchronous reference frame

$i_{gd,gq}$ are dq component of grid side current changed to synchronous reference frame

From equation (2.9), on solving grid side current (GSC) i_{gd} and i_{gq} are given as

$$\begin{bmatrix} i_{gd} \\ i_{gq} \end{bmatrix} = K_v \begin{bmatrix} p_g(t) \\ q_g(t) \end{bmatrix} \quad (2.10)$$

Where,

$$K_v = \frac{2}{3 |v_s|^2} \begin{bmatrix} v_{sd} & v_{sq} \\ v_{sq} & -v_{sd} \end{bmatrix}$$

and

$$|v_s| = \sqrt{|v_{sd}|^2 + |v_{sq}|^2}$$

Similarly, the instantaneous real power, $p_s(t)$ and reactive power , $q_s(t)$ components of Doubly Fed Induction Generator (DFIG) is :

$$\begin{bmatrix} p_s(t) \\ q_s(t) \end{bmatrix} = -\frac{3}{2} \begin{bmatrix} v_{sd} & v_{sq} \\ v_{sq} & -v_{sd} \end{bmatrix} \begin{bmatrix} i_{sd} \\ i_{sq} \end{bmatrix} \quad (2.11)$$

From this the stator current i_{sd} and i_{sq} are calculated as:

$$\begin{bmatrix} i_{sd} \\ i_{sq} \end{bmatrix} = -K_v \begin{bmatrix} p_s(t) \\ q_s(t) \end{bmatrix} \quad (2.12)$$

The minus sign in (2.12) goes along the bearing of the stator force stream as DFIG offering supply to Grid.

2.3 Modelling of DFIG Using Power Components:

The stator and rotor, flux and voltage equations of a DFIG in the stator voltage in synchronous reference frame are given as:[3]

$$v_{sdq} = r_s i_{sdq} + j\omega_e \psi_{sdq} + \frac{d\psi_{sdq}}{dt} \quad (2.13)$$

$$v_{rdq} = r_r i_{rdq} + j\omega_{sl} \psi_{rdq} + \frac{d\psi_{rdq}}{dt} \quad (2.14)$$

$$\psi_{sdq} = L_s i_{sdq} + L_m i_{rdq} \quad (2.15)$$

$$\psi_{rdq} = L_r i_{rdq} + L_m i_{sdq} \quad (2.16)$$

Where r_s = stator resistance

r_r =rotor resistance

‘s’ and ‘r’ stands for the stator and rotor variable respectively.

L_s = stator inductance

L_m =magnetizing inductance

L_r =rotor inductances

ω_r = rotor speed of the induction machine

ω_{sl} =slip frequency

$$\omega_{sl} = \omega_e - \omega_r$$

v_{sdq} =stator voltage in dq reference frame

$$v_{sdq} = v_{sd} + jv_{sq}$$

v_{rdq} =rotor voltage in dq reference frame

$$v_{rdq} = v_{rd} + jv_{rq}$$

i_{sdq} =stator current in dq reference frame

$$i_{sdq} = i_{sd} + j i_{sq}$$

i_{rdq} =rotor current in dq reference frame

$$i_{rdq} = i_{rd} + j i_{rq}$$

ψ_{sdq} = stator flux in dq reference frame

$$\psi_{sdq} = \psi_{sd} + j\psi_{sq}$$

ψ_{rdq} = rotor flux in dq reference frame

$$\psi_{rdq} = \psi_{rd} + j\psi_{rq}$$

Now , To get a model of DFIG using active and reactive power, the rotor current will be from equation (2.15) as:

$$i_{rdq} = \frac{\psi_{sdq} - L_s i_{sdq}}{L_m} \quad (2.17)$$

and from equation (2.16) and (2.17), rotor flux is given as:

$$\psi_{rdq} = \frac{L_r}{L_m} (\psi_{sdq} - L_s' i_{sdq}) \quad (2.18)$$

Where $L_s' = \left(1 - \frac{L_m^2}{L_s L_r}\right) L_s$

Now, by substituting i_{rdq} from equation (2.15) in equation (2.14) and then solving equation (2.13) and (2.14) for i_{sdq} , we get:

$$\frac{d(i_{sdq})}{dt} = \frac{1}{L_s'} v_{sdq} - \frac{L_m}{L_s' L_r} v_{rdq} + \frac{r_r - j\omega_r L_r}{L_s' L_r} \psi_{sdq} + \left(\frac{r_r L_s + r_s L_r}{L_s' L_r} + j\omega_{sl} \right) i_{sdq} \quad (2.19)$$

From equation (2.12), substituting i_{sd} , i_{sq} components of i_{sdq} in equation (2.19) and solve it in term of p_s and q_s :

$$\frac{d(p_s(t))}{dt} = g_1 p_s - \omega_{sl} q_s - g_4 \psi_{sd} - g_5 \psi_{sq} + u_{rd} \quad (2.20)$$

$$\frac{d(q_s(t))}{dt} = \omega_{sl} p_s + g_1 q_s - g_5 \psi_{sd} + g_4 \psi_{sq} + u_{rq} \quad (2.21)$$

Where

$$u_{rd} = g_2 v_{rd} + g_3 v_{rq} - \frac{3 |v_s|^2}{2 L_s'} \quad (2.22)$$

$$u_{rq} = g_3 v_{rd} - g_2 v_{rq} \quad (2.23)$$

$$g_1 = - \frac{r_r L_s + r_s L_r}{L_s' L_r}$$

$$g_2 = \frac{3 L_m v_{sd}}{2 L_s' L_r}$$

$$g_3 = \frac{3 L_m v_{sq}}{2 L_s' L_r}$$

$$g_4 = \frac{3}{2} \left(\frac{r_r v_{sd} - L_r \omega_r v_{sq}}{L_s' L_r} \right)$$

$$g_5 = \frac{3}{2} \left(\frac{r_r v_{sq} + L_r \omega_r v_{sd}}{L_s' L_r} \right)$$

Solving the stator voltage equations for ψ_{sdq}

$$\frac{d(\psi_{sd})}{dt} = v_{sd} + \omega_e \psi_{sq} + \frac{2 r_s}{3 |v_s|^2} (v_{sd} p_s + v_{sq} q_s) \quad (2.24)$$

$$\frac{d(\psi_{sq})}{dt} = v_{sq} - \omega_e \psi_{sd} + \frac{2 r_s}{3 |v_s|^2} (v_{sq} p_s - v_{sd} q_s) \quad (2.25)$$

The machine's electromechanical dynamic model is given as:

$$\frac{d \omega_r}{dt} = \frac{P}{J} (T_e - T_m) \quad (2.26)$$

P= No. of pole pairs

J= Rotor inertia

T_m = input mechanical torque of the machine

T_e =electrical torque of the machine

The electrical torque developed in the machine is given by:

$$T_e = \frac{3P}{2} (\psi_{sd} i_{sq} - \psi_{sq} i_{sd}) \quad (2.27)$$

By substituting for i_{sd} and i_{sq} from equation (2.12) in equation (2.26) and then putting the value of T_e in equation (2.27), then we get:

$$\frac{d\omega_r}{dt} = g_6 p_s + g_7 q_s - \frac{P}{J} T_m \quad (2.28)$$

Where

$$g_6 = \frac{P^2}{J} \left(\frac{\psi_{sq} v_{sd} - \psi_{sd} v_{sq}}{|v_s|^2} \right)$$

$$g_7 = \frac{P^2}{J} \left(\frac{\psi_{sd} v_{sd} + \psi_{sq} v_{sq}}{|v_s|^2} \right)$$

The Matrix model of the Doubly-Fed induction machine is shown below in state variable matrix form is obtained from equation (2.20) to (2.25) and (2.28), is given as:

$$\frac{d}{dx} \begin{bmatrix} p_s \\ q_s \\ \psi_{sd} \\ \psi_{sq} \\ \omega_r \end{bmatrix} = \begin{bmatrix} g_1 & -\omega_{sl} & -g_4 & -g_5 & 0 \\ \omega_{sl} & g_1 & -g_5 & g_4 & 0 \\ \frac{2r_s v_{sd}}{3|v_s|^2} & \frac{2r_s v_{sq}}{3|v_s|^2} & 0 & \omega_e & 0 \\ \frac{2r_s v_{sq}}{3|v_s|^2} & \frac{-2r_s v_{sd}}{3|v_s|^2} & -\omega_e & 0 & 0 \\ g_6 & g_7 & 0 & 0 & 0 \end{bmatrix} \begin{bmatrix} p_s \\ q_s \\ \psi_{sd} \\ \psi_{sq} \\ \omega_r \end{bmatrix} + \begin{bmatrix} u_{rd} \\ u_{rq} \\ v_{sd} \\ v_{sq} \\ -\frac{P^2}{J} T_m \end{bmatrix} \quad (2.29)$$

The above model of DFIG we got, is a nonlinear dynamic model because the coefficients of the matrix input are functions of the state variables.

2.4 Modelling of Grid-Side Converter and filter

The equivalent circuit diagram of GSF in the synchronous reference frame is shown below.

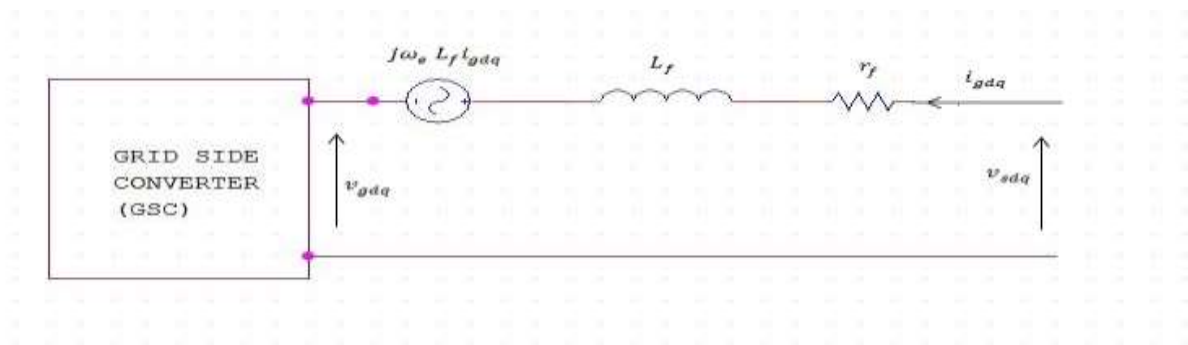


Fig 2.3 Equivalent circuit diagram of grid side filter

The model of the grid-side converter and filter in dq reference frame is given as: [3]

$$v_{sdq} = v_{gdq} + r_f i_{gdq} + j\omega_e L_f i_{gdq} + L_f \frac{d i_{gdq}}{dt} \quad (2.30)$$

Here subscript "g" means the variables at the network side converter.

Where, r_f = resistance of the filter

L_f = inductance of filter

From equation (2.10), substituting i_{gd} , i_{gq} components of i_{gdq} in equation (2.30) and solve in term of p_g and q_g , we obtain:

$$\frac{d}{dt} \begin{bmatrix} p_g(t) \\ q_g(t) \end{bmatrix} = \begin{bmatrix} -\frac{r_f}{L_f} & -\omega_e \\ \omega_e & -\frac{r_f}{L_f} \end{bmatrix} \begin{bmatrix} p_g(t) \\ q_g(t) \end{bmatrix} + \begin{bmatrix} u_{gd} \\ u_{gq} \end{bmatrix} \quad (2.31)$$

Where

$$u_{gd} = \frac{3}{2L_f} (|v_s|^2 - (v_{sd} v_{gd} + v_{sq} v_{gq})) \quad (2.32)$$

$$u_{gq} = \frac{3}{2L_f} (v_{gq} v_{sd} - v_{gd} v_{sq}) \quad (2.33)$$

The dc-link model is obtained as:

$$V_{dc}(t) I_{dc}(t) = p_g(t) - p_r(t) - p_{loss}(t) \quad (2.34)$$

Where, $p_g(t)$ = the real power that converter gives to the rotor
 $p_{loss}(t)$ = total power loss of the filter

$p_r(t)$ is the rotor power

The real power to the rotor is:

$$p_r(t) = \frac{3}{2} (v_{rd} i_{rd} + v_{rq} i_{rq}) \quad (2.35)$$

From equation (2.17) and (2.12), p_r is expressed as:

$$p_r = \frac{L_s}{L_m} \left(\frac{v_{sd} v_{rd} + v_{sq} v_{rq}}{|v_s|^2} \right) p_s + \frac{L_s}{L_m} \left(\frac{v_{sq} v_{rd} - v_{sd} v_{rq}}{|v_s|^2} \right) q_s + \frac{3 v_{rd}}{2L_m} \psi_{sd} + \frac{3 v_{rq}}{2L_m} \psi_{sq} \quad (2.36)$$

Since dc link current expression is given by:

$$I_{dc}(t) = C \frac{d V_{dc}(t)}{dt}$$

In equation (2.34) by substituting the value of dc link model is deduced as : [3]

$$\frac{d V_{dc}(t)}{dt} = \frac{I_{dc}(t)}{C} = \frac{p_g(t) - p_r(t)}{C V_{dc}} \quad (2.37)$$

2.5 Model OF Wind Turbine

The mechanical power extracted by a wind turbine is expressed as

$$P_m = \frac{1}{2} C_p(\lambda, \beta) \pi R^2 \rho V_w^3 \quad (2.38)$$

Where R= Radius of wind turbine

ρ = density of air mass

V_w = wind speed

C_p = wind turbine power coefficient which is a dependent of TSR and pitch angle β of the turbine

$$\text{Tip speed ratio } (\lambda) = \frac{R\omega}{V_w}$$

Power output coefficient C_p is related to of tip speed ratio (TSR) and pitch angle β of the wind turbine blade as the following expression:

$$C_p(\lambda, \beta) = C_1 \left(\frac{C_2}{\lambda_i} - C_3\beta - C_4 \right) e^{\left(\frac{C_5}{\lambda_i} \right)} + C_6\lambda \quad (2.39)$$

where

$$\frac{1}{\lambda_i} = \frac{1}{(\lambda + 0.08\beta)} - \frac{0.035}{(\lambda^3 + 1)}$$

From experimentally it is found that $C_1 = 0.5176$; $C_2 = 116$; $C_3 = 0.4$; $C_4 = 5$; $C_5 = 21$; and $C_6 = 0.0068$

For a high-rating wind turbine, the maximum mechanical power extracted at optimum values of TSR λ_{opt} in range of 5 to 8. It is shown that $C_p < 0.6$ and the maximum value of C_p is

0.5926 which is Betz limit. Practically for an optimum value of TSR, power coefficient C_p is considered about 0.51 for high-rating wind turbines system.

2.6 Linearization of model of a DFIG machine –

For a high-rating machine, the stator resistant is very small ,hence a constant stator voltage under symmetrical operation gives slow-changing flux components.

So, dq components for the stator flux in field-oriented frame of reference for DFIG are given by considering $v_{sq} = 0$ as:[3]

$$\begin{aligned} \psi_{sd} &= 0 \quad \text{and} \\ \psi_{sq} &= -\frac{v_{sd}}{\omega_e} \end{aligned} \quad (2.40)$$

From equation (2.40) substituting the values of in equation (2.20),(2.21) and (2.28), then the equations are linearized about an operating point ,so, the small-signal model of machine is represented as :

$$\frac{d \tilde{p}_s}{dt} = -g_1 \tilde{p}_s - \omega_{slo} \tilde{q}_s + (q_{s0} + g_8) \tilde{\omega}_r + \tilde{u}_{rd} \quad (2.41)$$

$$\frac{d \tilde{q}_s}{dt} = \omega_{slo} \tilde{p}_s - g_1 \tilde{q}_s - p_{s0} \tilde{\omega}_r + \tilde{u}_{rq} \quad (2.42)$$

$$\frac{d \tilde{\omega}_r}{dt} = -\frac{p^2}{J \omega_e} \tilde{p}_s - \frac{p}{J} \tilde{T}_m \quad (2.43)$$

Where

$$g_8 = \frac{3 v_{sd}^2}{2 L_s' \omega_e}$$

Where, tilde ~ denotes small-signal quantities.

Here, the superscript ‘0’ says the quantities at an operating point .

Power and torque equation : $P_m = T_m \omega_r$

The power and torque equation is linearized by taking wind speed is constant as

$$\tilde{T}_m = K_T \tilde{\omega}_r \quad (2.44)$$

Where K_T is obtained by linearizing P_m as:

$$K_T = \left(\frac{1}{2} \pi R^2 \rho V_{w0}^3 \right) \left(\frac{R}{V_{w0} \omega_{r0}} \left(\frac{\partial C_p}{\partial \lambda} \right)_{\lambda_0} - \frac{C_{p0}}{\omega_{r0}^2} \right)$$

By Laplace transform of dynamic model of DFIG and wind turbine, we will get:

$$\begin{bmatrix} s + g_1 & \omega_{sl0} & -(q_{s0} + g_8) \\ -\omega_{sl0} & s + g_1 & p_{s0} \\ \frac{p^2}{J\omega_e} & 0 & s + \frac{PK_T}{J} \end{bmatrix} \begin{bmatrix} \tilde{p}_s \\ \tilde{q}_s \\ \tilde{\omega}_r \end{bmatrix} = \begin{bmatrix} \tilde{u}_{rd} \\ \tilde{u}_{rq} \\ 0 \end{bmatrix} \quad (2.45)$$

$$\text{Where,} \quad \tilde{u}_{rd} = g_2 \tilde{v}_{rd} \quad \text{and} \quad \tilde{u}_{rq} = -g_2 \tilde{v}_{rq}$$

From equation (2.45), In Laplace domain, the dynamic model of DFIG and the wind turbine model is expressed based on a power transfer function as below:

$$\begin{bmatrix} \tilde{p}_s \\ \tilde{q}_s \\ \tilde{\omega}_r \end{bmatrix} = \begin{bmatrix} h_{11} & h_{12} \\ h_{21} & h_{22} \\ h_{31} & h_{32} \end{bmatrix} \begin{bmatrix} \tilde{u}_{rd} \\ \tilde{u}_{rq} \end{bmatrix} \quad (2.46)$$

The grid-side filter modelling in Laplace domain done by substituting equation (2.31), into the Laplace domain and expressed as:

$$\begin{bmatrix} s + \frac{r_f}{L_f} & \omega_e \\ \omega_e & s + \frac{r_f}{L_f} \end{bmatrix} \begin{bmatrix} \tilde{p}_g \\ \tilde{q}_g \end{bmatrix} = \begin{bmatrix} \tilde{u}_{gd} \\ \tilde{u}_{gq} \end{bmatrix} \quad (2.47)$$

Where

$$\tilde{u}_{gd} = -\frac{3 v_{sd}}{2 L_f} \tilde{v}_{gd} \quad (2.48)$$

$$\tilde{u}_{gq} = \frac{3 v_{sd}}{2 L_f} \tilde{v}_{gq} \quad (2.49)$$

from equation (2.47), on solving for \widetilde{p}_g and \widetilde{q}_g the GSF model in the Laplace domain is given by:

$$\begin{bmatrix} \widetilde{p}_g \\ \widetilde{q}_g \end{bmatrix} = \begin{bmatrix} g_{11} & g_{12} \\ g_{21} & g_{22} \end{bmatrix} \begin{bmatrix} \widetilde{u}_{gd} \\ \widetilde{u}_{gq} \end{bmatrix} \quad (2.50)$$

Where

from equation (2.27), the linearized model of dc link is given by:

$$\frac{d \widetilde{V}_{dc}}{dt} = \frac{\widetilde{p}_g - \widetilde{p}_r}{C V_{dc0}} \quad (2.51)$$

Where

$$\widetilde{p}_r = \alpha_1 \widetilde{p}_s + \alpha_2 \widetilde{q}_s + \alpha_3 \widetilde{u}_{rd} + \alpha_4 \widetilde{u}_{rq} \quad (2.52)$$

From equation (2.34), dc link model in the Laplace domain is given by:

$$\widetilde{V}_{dc} = \frac{\widetilde{p}_g - \widetilde{p}_r}{sC V_{dc0}} \quad (2.53)$$

2.7 Free acceleration characteristics of Induction machine-

For analysis of induction machines during no load condition which is also known as free Acceleration mode of machine from stall, there is need of study of relationship between torque and speed. For this purpose free acceleration of the squirrel cage induction machine are simulated on MATLAB and studies are performed. [6]

CHAPTER-3

CONTROL STRATEGY OF DFIG WIND TURBINE

3.1 Sequential loop closing (SLC):

The sequential loop closing (SLC) scheme is also known as multi-loop control method that is used for multivariable control processes. In this Scheme, each controller is sequentially designed from the transfer function of every pair of inputs and outputs considering the former controllers is a part of it and closed. In it, the single-input single-output (SISO) auto-tuning technique is used. The transfer function of the latter pair of inputs and outputs is varied considerably as the former loops are closed. [14]

3.2 Design of control system for a DFIG wind turbine system:

3.2.1 Controller Design Method:

Converters of Machine side and grid side control system is shown as below in the figure3.1. The multiple loop closing (SLC) scheme is taken for modelling six controllers. [14,15]

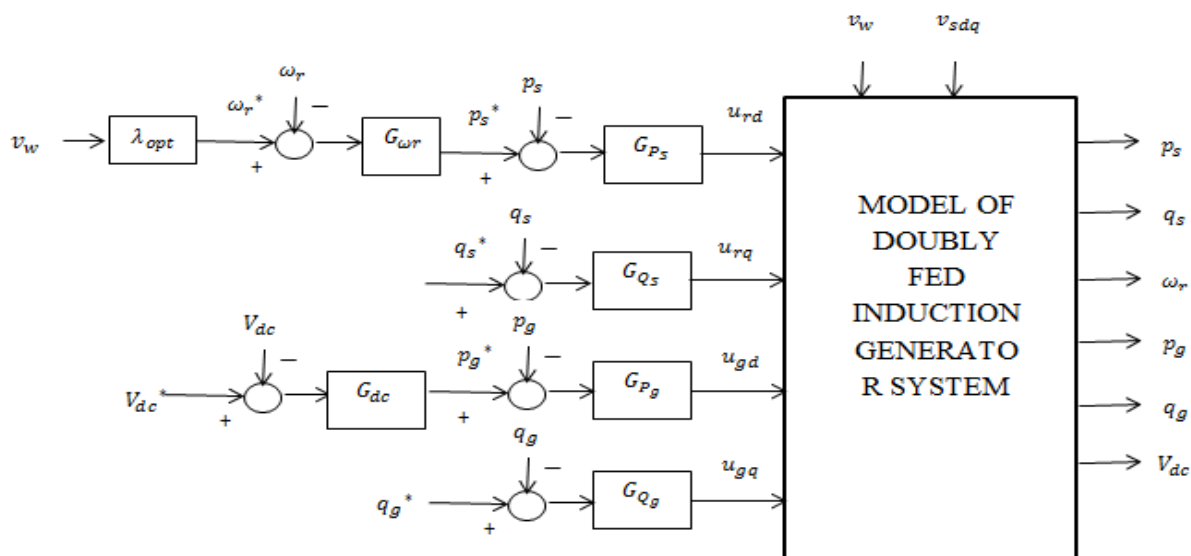


Fig.3.1 diagram of the rotor-side and grid-side converter controller

3.2.2 Rotor-Side Controller design

Stator Reactive and Active Power Controllers Design:

By taking $(\tilde{u}_{rd}, \tilde{p}_s)$ as the 1st input- output equation (2.47) and

Imposing $u_{rq} = 0$, we derived the first SISO subsystem for controller design as:

$$\tilde{p}_s = h_{11} \tilde{u}_{rd} \quad (3.1)$$

The first controller is designed as:

$$\tilde{u}_{rd} = G_{P_s} (\tilde{p}_s^* - \tilde{p}_s) \quad (3.2)$$

From equation (3.1) and (3.2) the closed-loop design of the 1st subsystem in Laplace mode is given as:

$$\tilde{p}_s = \frac{h_{11} G_{P_s}}{1+h_{11} G_{P_s}} \tilde{p}_s^* \quad (3.3)$$

All the poles of G_{P_s} should be lie left to the imaginary axis of s plane

$$\tilde{u}_{rd} = G_{P_s} (\tilde{p}_s^* - \tilde{p}_s)$$

and

$$\tilde{u}_{rq} = G_{Q_s} (\tilde{q}_s^* - \tilde{q}_s)$$

from equation (2.46), the closed-loop model of the 2nd subsystem is given by:

$$\tilde{p}_s = \frac{G_1}{1+G_2 G_{Q_s}} \tilde{p}_s^* + \frac{G_1 G_{Q_s}}{1+G_2 G_{Q_s}} \tilde{q}_s^* \quad (3.4)$$

where

$$G_1 = \frac{h_{21} G_{P_s}}{1 + h_{11} G_{P_s}}$$

$$G_2 = h_{22} - \frac{h_{12} h_{21} G_{P_s}}{1 + h_{11} G_{P_s}}$$

So controller G_{Q_s} should be designed as the second subsystem in equation (3.4) remains stable.

3.2.3 Controller design for Rotor speed

Control of the speed of the turbine-generator rotor is performed by controlling active stator power. Thus, the speed controller G_{ω_r} considers \widetilde{p}_s^* as controller input. From the control scheme \widetilde{p}_s^* is given as:

$$\widetilde{p}_s^* = G_{\omega_r} (\widetilde{\omega}_r^* - \widetilde{\omega}_r) \quad (3.5)$$

By embedding G_{P_s} and G_{Q_s} controllers in the system model, the of rotor speed transfer function is calculated as :

$$\widetilde{\omega}_r = G_3 \widetilde{p}_s^* + G_4 \widetilde{q}_s^* \quad (3.6)$$

Where,

$$G_3 = \frac{h_{31} G_{P_s} (1 + G_{Q_s} (G_1 + G_2))}{(1 + h_{11} G_{P_s}) (1 + G_2 G_{Q_s})} - \frac{h_{31} G_1 G_{Q_s}}{1 + G_2 G_{Q_s}}$$

$$G_4 = \frac{h_{32} G_{Q_s}}{1 + G_2 G_{Q_s}} - \frac{h_{12} h_{31} G_{P_s}^2}{(1 + h_{11} G_{P_s}) (1 + G_2 G_{Q_s})}$$

After Substituting \widetilde{p}_s^* from equation (3.5) in equation (3.6) and solving for $\widetilde{\omega}_r$ we get

$$\widetilde{\omega}_r = \frac{G_3 G_{\omega_r}}{1 + G_3 G_{\omega_r}} \widetilde{\omega}_r^* + \frac{G_4}{1 + G_3 G_{\omega_r}} \widetilde{q}_s^* \quad (3.7)$$

So controller G_{ω_r} should be designed so that the second subsystem in equation (3.7) remains stable.

3.2.4 Controller Design for Grid Side:

Grid-Side Reactive and Active Power Controllers Design:

By taking $(\widetilde{u}_{gd}, \widetilde{p}_g)$ as the 1st input- output couple in equation (2.50) and

Imposing $u_{gq} = 0$, we get the 1st SISO subsystem for design of controller as:

$$\widetilde{p}_g = g_{11} \widetilde{u}_{gd} \quad (3.8)$$

The first controller is designed as:

$$\tilde{u}_{gd} = G_{Pg} (\widetilde{p}_g^* - \widetilde{p}_g) \quad (3.9)$$

From equation (3.8) and (3.9) the closed-loop design of the first subsystem in Laplace system is given as:

$$\widetilde{p}_g = \frac{g_{11} G_{Pg}}{1 + g_{11} G_{Pg}} \widetilde{p}_g^* \quad (3.10)$$

Thus G_{Pg} must be designed so that all poles of equation (3.10) stay in the left-half plane of s-plane. The model of G_{Pg} is performed by considering SISO design methods, such as frequency response or root locus.

$$\tilde{u}_{gd} = G_{Pg} (\widetilde{p}_g^* - \widetilde{p}_g)$$

and

$$\tilde{u}_{gq} = G_{Qg} (\widetilde{q}_g^* - \widetilde{q}_g)$$

from equation (2.50), the feed back model for the 2nd subsystem is given by:

$$\widetilde{p}_g = \frac{G_{g1}}{1 + G_{g2} G_{Qg}} \widetilde{p}_g^* + \frac{G_{g1} G_{Qg}}{1 + G_{g2} G_{Qg}} \widetilde{q}_g^* \quad (3.11)$$

where

$$G_{g1} = \frac{g_{21} G_{Pg}}{1 + g_{11} G_{Pg}}$$

$$G_{g2} = g_{22} - \frac{g_{12} g_{21} G_{Pg}}{1 + g_{11} G_{Pg}}$$

So controller G_{Qg} should be modelled as 2nd subsystem in equation (3.11) remains stable.

3.2.5 DC-Link Voltage Controller Design:

In equation (2.52) by substituting the values \widetilde{p}_s , \widetilde{q}_s , \tilde{u}_{rd} and \tilde{u}_r on solving we get:

$$\widetilde{p}_r = \frac{G_5 G_{\omega_r}}{1 + G_3 G_{\omega_r}} \widetilde{\omega}_r^* + \left(G_6 - \frac{G_3 G_5 G_{\omega_r}}{1 + G_3 G_{\omega_r}} \right) \widetilde{q}_s^* \quad (3.12)$$

In the system, \widetilde{p}_g^* controls at its reference value controlling the dc-link controller G_{dc} as :

$$\widetilde{p}_g^* = G_{dc}(\widetilde{V}_{dc}^* - \widetilde{V}_{dc})$$

Therefore, from equation (2.53) and (3.5) , the feed back system for \widetilde{V}_{dc} is shown as :

$$\widetilde{V}_{dc} = \frac{G_7 G_{dc} \widetilde{V}_{dc}^* + G_8 \widetilde{q}_s^*}{s C V_{dc0} + G_7 G_{dc}} - \frac{G_5 G_{\omega_r} \widetilde{\omega}_r^* + (G_6 + G_3 G_{\omega_r} (G_6 - G_5)) \widetilde{q}_s^*}{(s C V_{dc0} + G_7 G_{dc})(1 + G_3 G_{\omega_r})} \quad (3.13)$$

Where

$$G_5 = \frac{G_1(\alpha_2 - \alpha_4 G_{Q_s})}{1 + G_2 G_{Q_s}} + \alpha_3 G_{P_s} + \frac{(\alpha_1 - \alpha_3 G_{P_s})(h_{11} G_{P_s}(1 + G_2 G_{Q_s}) - h_{12} G_1 G_{Q_s})}{(1 + h_{11} G_{P_s})(1 + G_2 G_{Q_s})}$$

$$G_6 = \frac{h_{12} G_{P_s}(\alpha_1 - \alpha_3 G_{P_s})}{(1 + h_{11} G_{P_s})(1 + G_2 G_{Q_s})} + \frac{G_2 G_{Q_s}(\alpha_2 - \alpha_4 G_{Q_s})}{1 + G_2 G_{Q_s}} + \alpha_4 G_{Q_s}$$

$$G_7 = \frac{g_{21} G_{P_g}}{(1 + g_{11} G_{P_g})} \left(\frac{g_{11}}{g_{12}} + \frac{g_{21}}{g_{12}} G_8 \right)$$

$$G_8 = \frac{g_{12} G_{Q_g}}{1 + (g_{11} + g_{21}^2) G_{P_g} + g_{11} G_{Q_g} + g_{11}^2 G_{P_g} G_{Q_g}}$$

So controller G_{dc} should be modelled as 2nd subsystem in equation (3.13) remains stable.

3.3 Calculation of control Parameters

The system has been aconsidered as a 1.5-MW DFIG wind turbine-power source connected to grid. Using the described design method, the controllers are designed for the system developed are given :

$$G_{P_s} = 1.314 \left(1 + \frac{10}{s} + \frac{s}{165.15} \right) \left(\frac{1}{1 + 0.0154s} \right)$$

$$G_{Q_s} = 2.641 \left(1 + \frac{10}{s} + \frac{s}{330.255} \right) \left(\frac{1}{1 + 0.0328s} \right)$$

$$G_{P_g} = 2.641 \left(1 + \frac{10}{s} \right)$$

$$G_{Q_g} = 2.663 \left(1 + \frac{10}{s} \right)$$

$$G_{dc} = 4.51 \left(1 + \frac{2}{s} \right) G_{\omega_r} = 7.59 \left(1 + \frac{2}{s} \right)$$

CHAPTER-4

SIMULATIONS AND RESULTS

4.1 Design of Wind turbine

For a particular wind speed, power extraction from turbine will be maximum if the C_p will be maximum. For optimum value, the value of C_p will be maximum for a particular TSR value. With increased value of Pitch angle (β), the C_p decreases with increase in pitch angle with increasing TSR. The power output vs wind speed is also studied. The plot for C_p vs TSR is by varying the pitch angle to 0, 4 and 6.

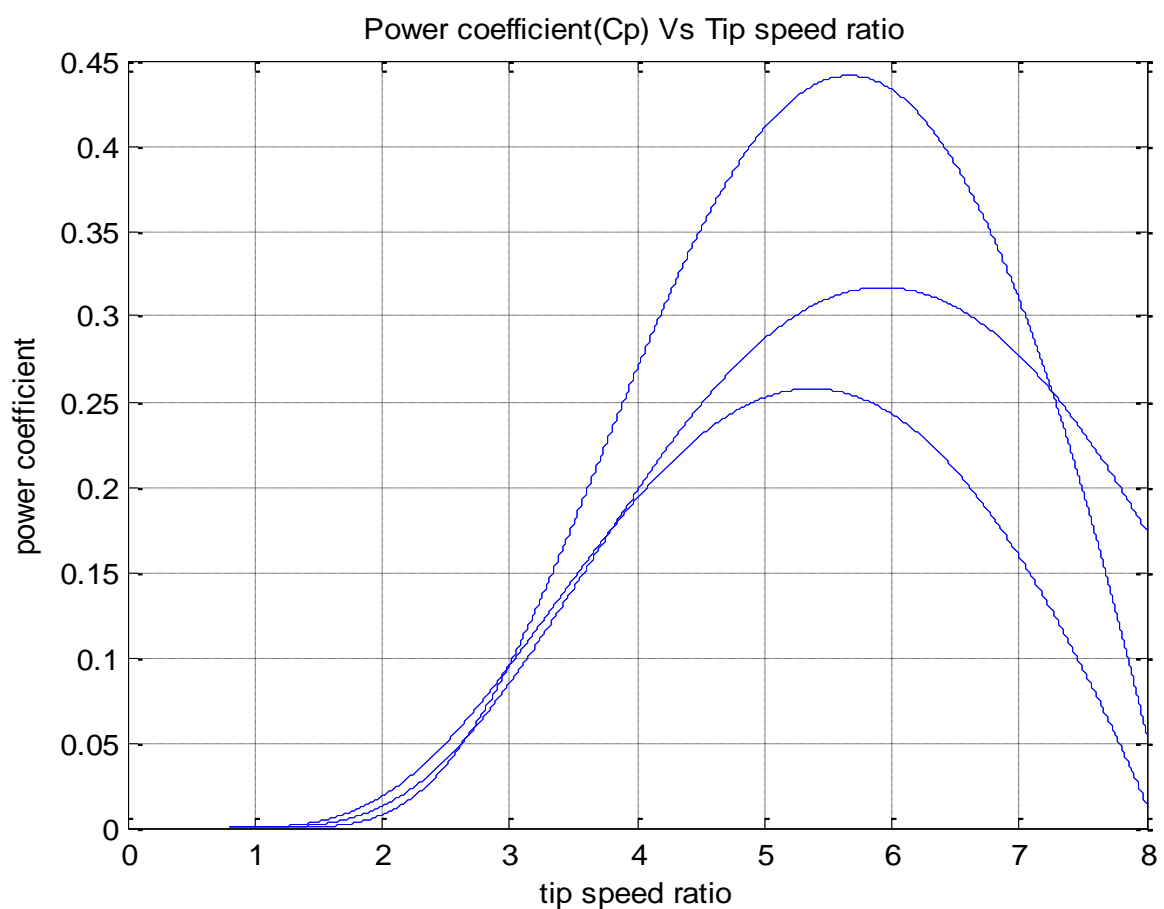


Fig.4.1(a) Power coefficient Vs Tip speed ratio characteristics

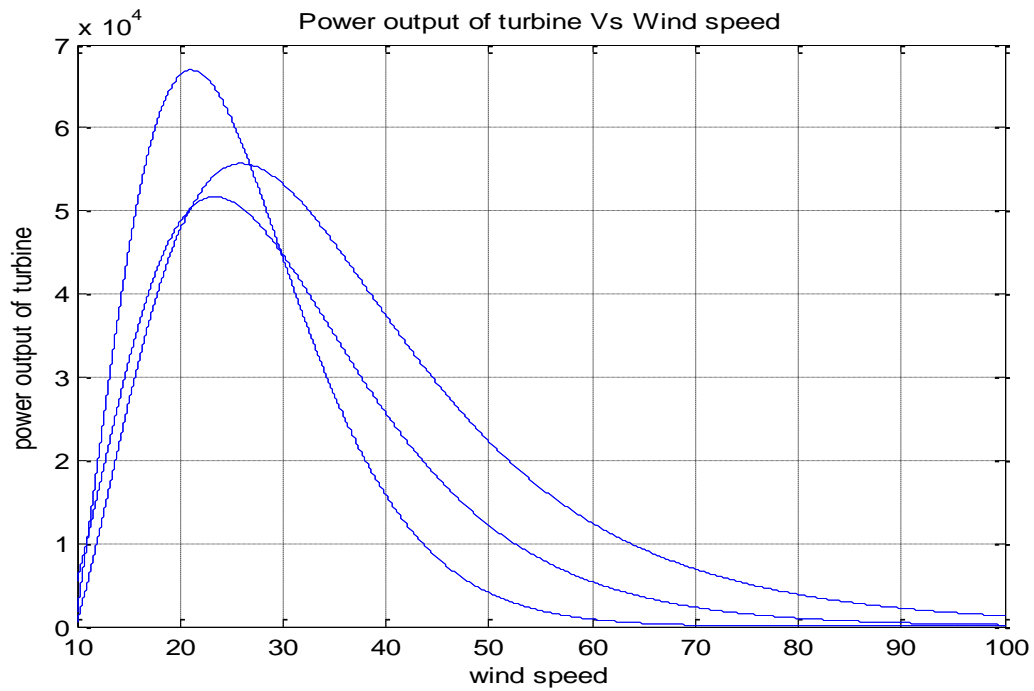


Fig 4.1(b)- Power output of turbine Vs Wind speed characteristics

4.2 Torque-Slip characteristics of Induction machine

The Torque-slip characteristics of Induction machine is plotted and It is seen that for slip in between 0 and 1 ($0 < s < 1$), the machine works in motoring mode whereas when the slip is negative ($s < 0$), the machine operates in Generating mode. The plot is done by varying the slip from -1 to 1. The characteristics is shown as below.

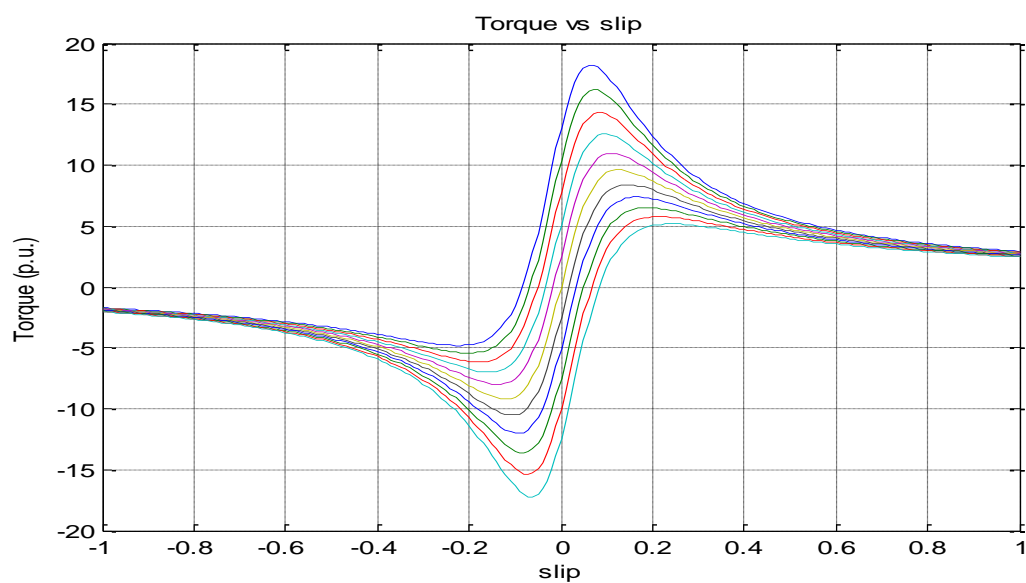


Fig 4.2- Torque vs speed characteristics

4.3 SIMULINK FOR CONTROLLING OF DFIG-

By applying Three phase supply to the machine through grid and after changing the variables to dq0 reference variables, and the plots for stator, rotor powers are plotted as below.

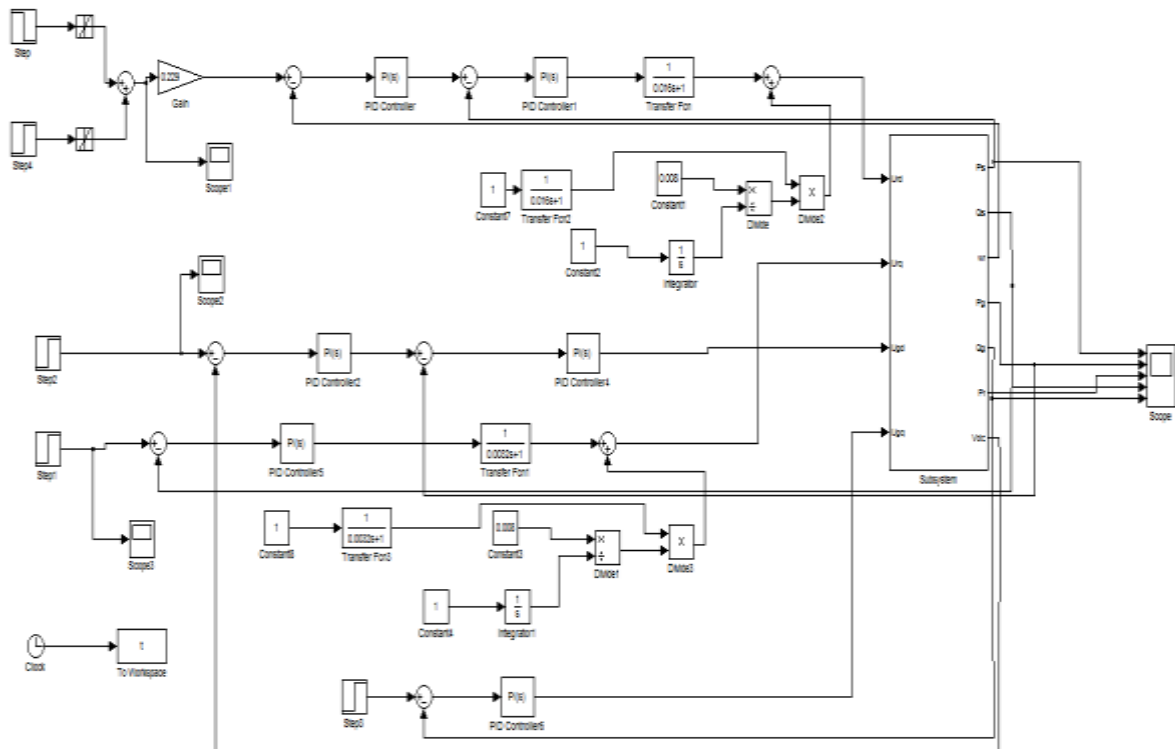


Fig.4.3 Simulink Block Diagram for controlling of DFIG

Waveforms-

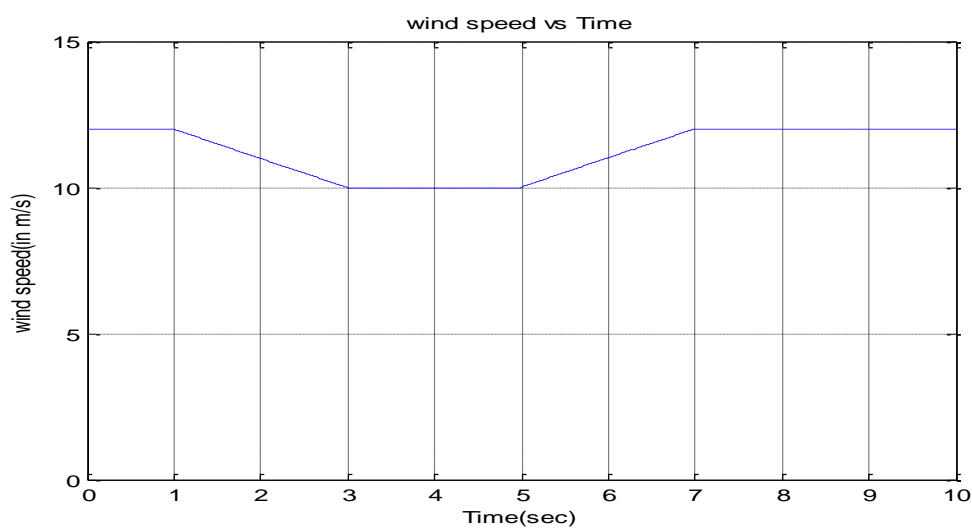


Fig.4.3.1 wind speed variation with time

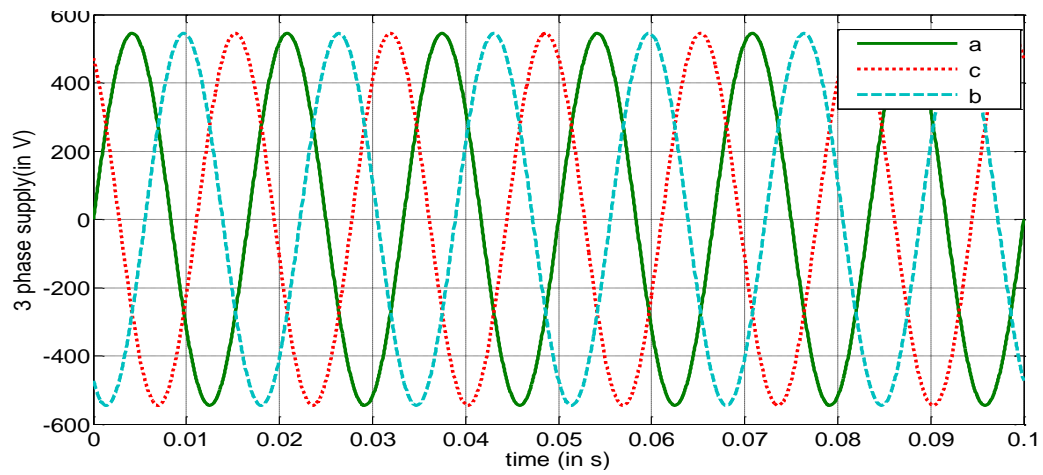


Fig 4.3.2 Three phase supply to stator

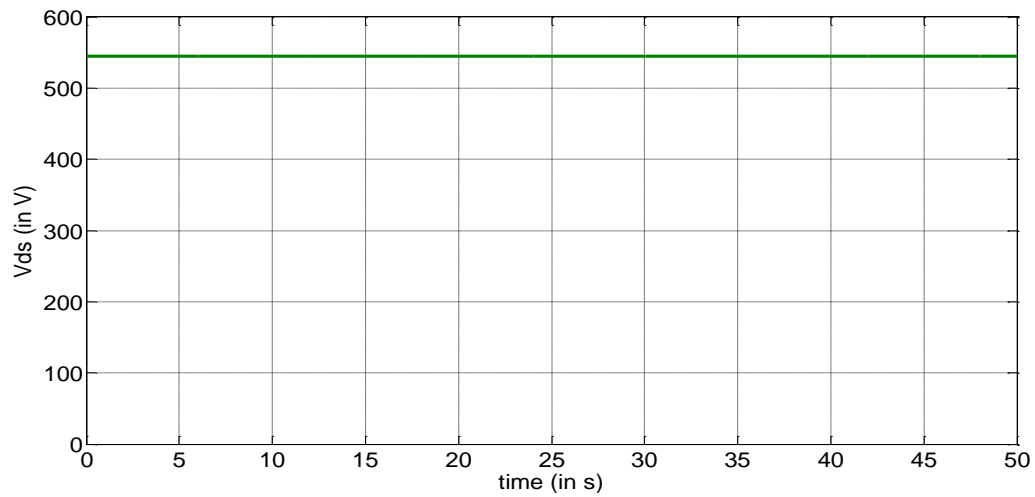


Fig 4.3.3 Stator voltage along d-axis

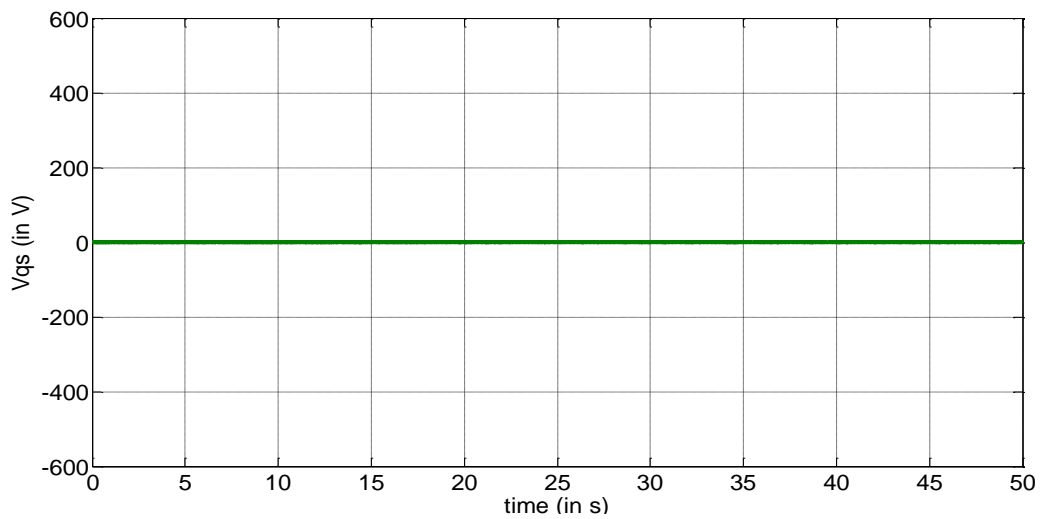


Fig 4.3.4 Stator voltage along q-axis

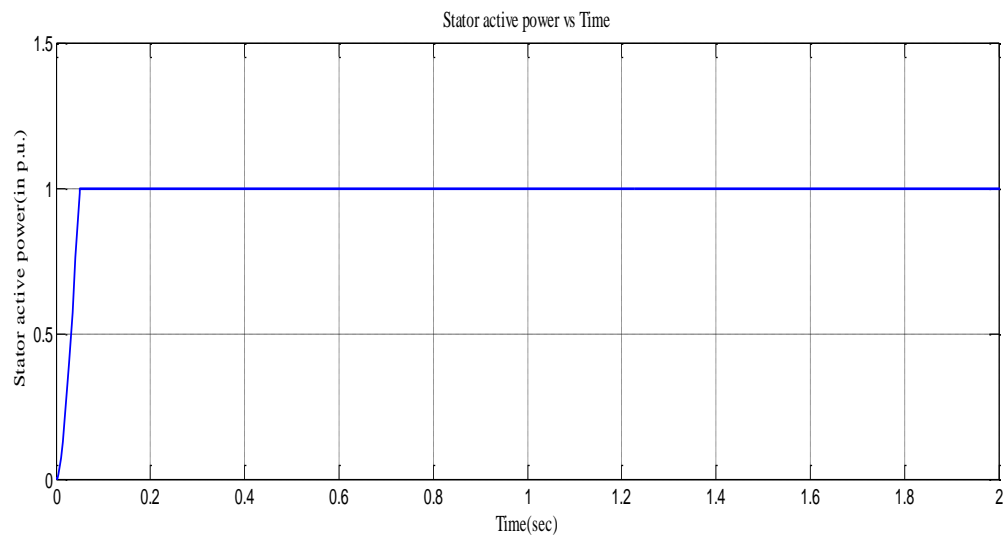


Fig 4.3.5 Stator active power

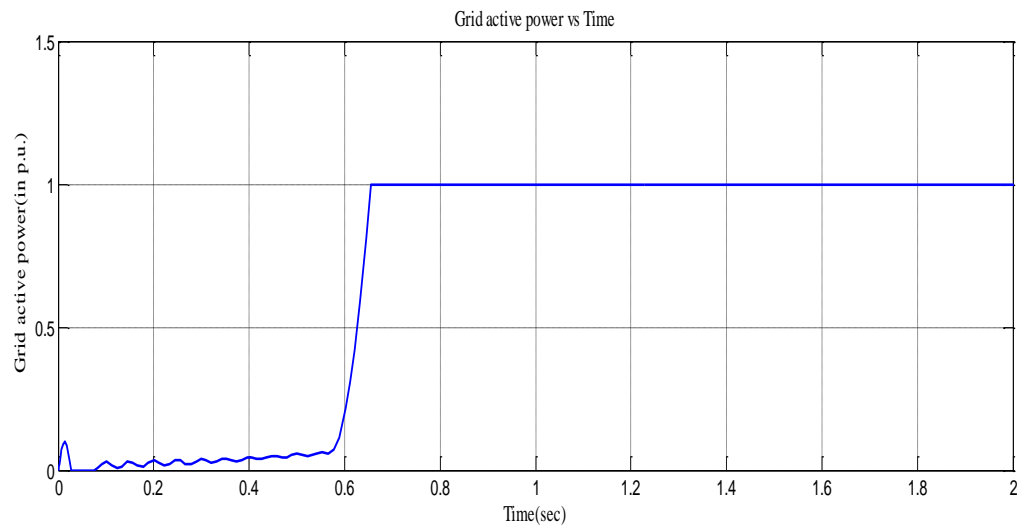


Fig 4.3.6 Grid-side active power

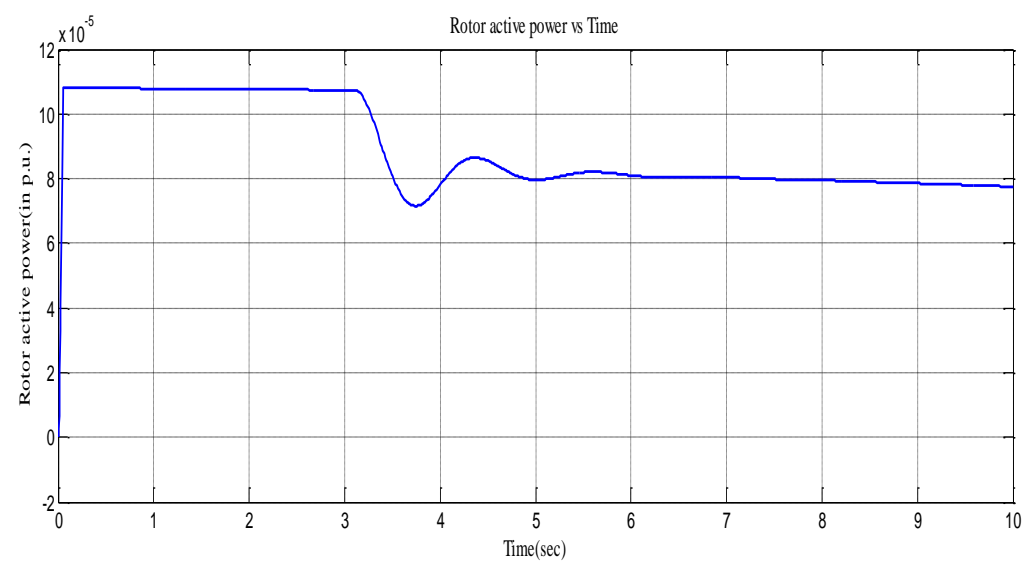


Fig 4.3.7 Rotor reactive power

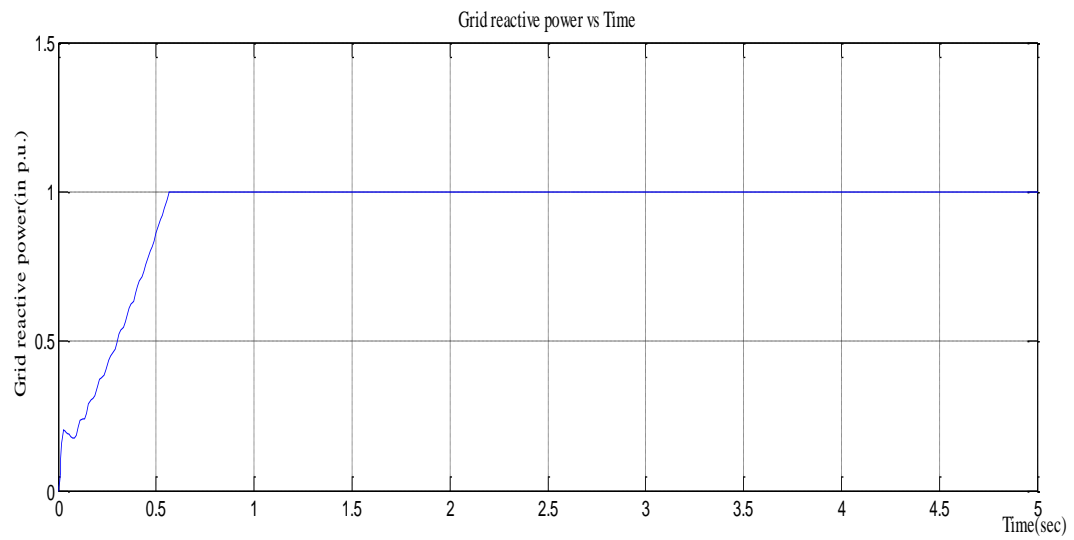


Fig 4.3.8 grid reactive power

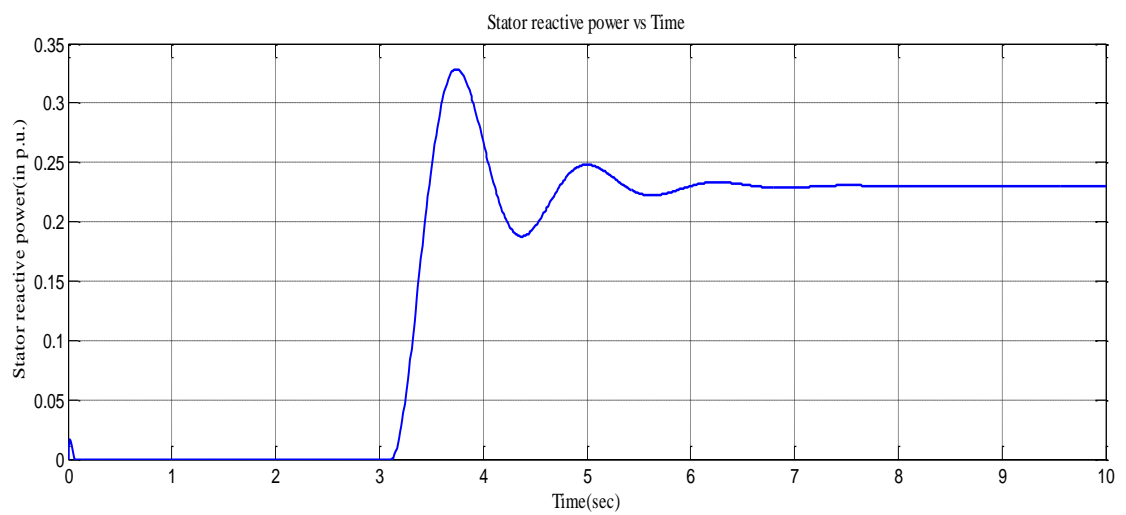


Fig 4.3.9 stator reactive power

4.4 Free Acceleration Characteristics For Induction Machine –

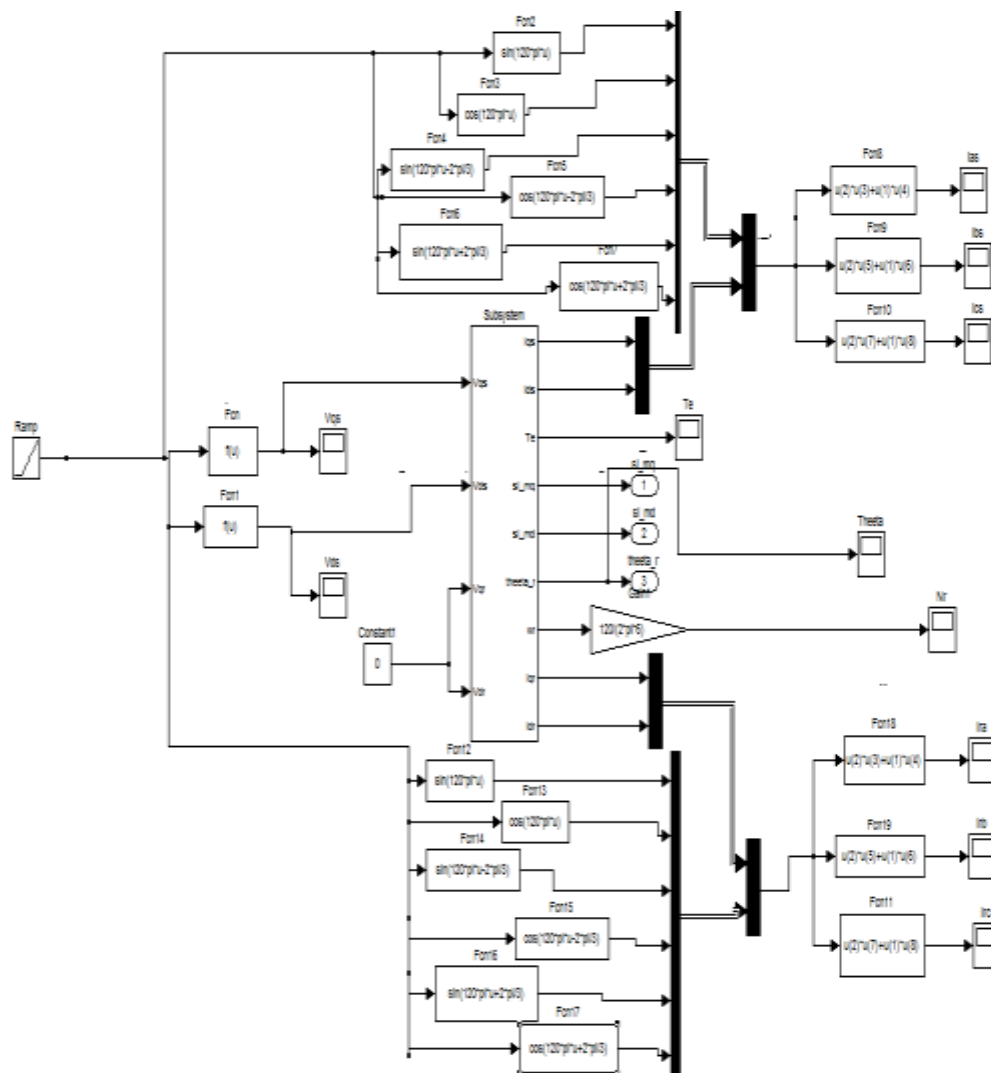


Fig 4.4.1- Simulink Block Diagram for Free acceleration characteristics of Induction machine

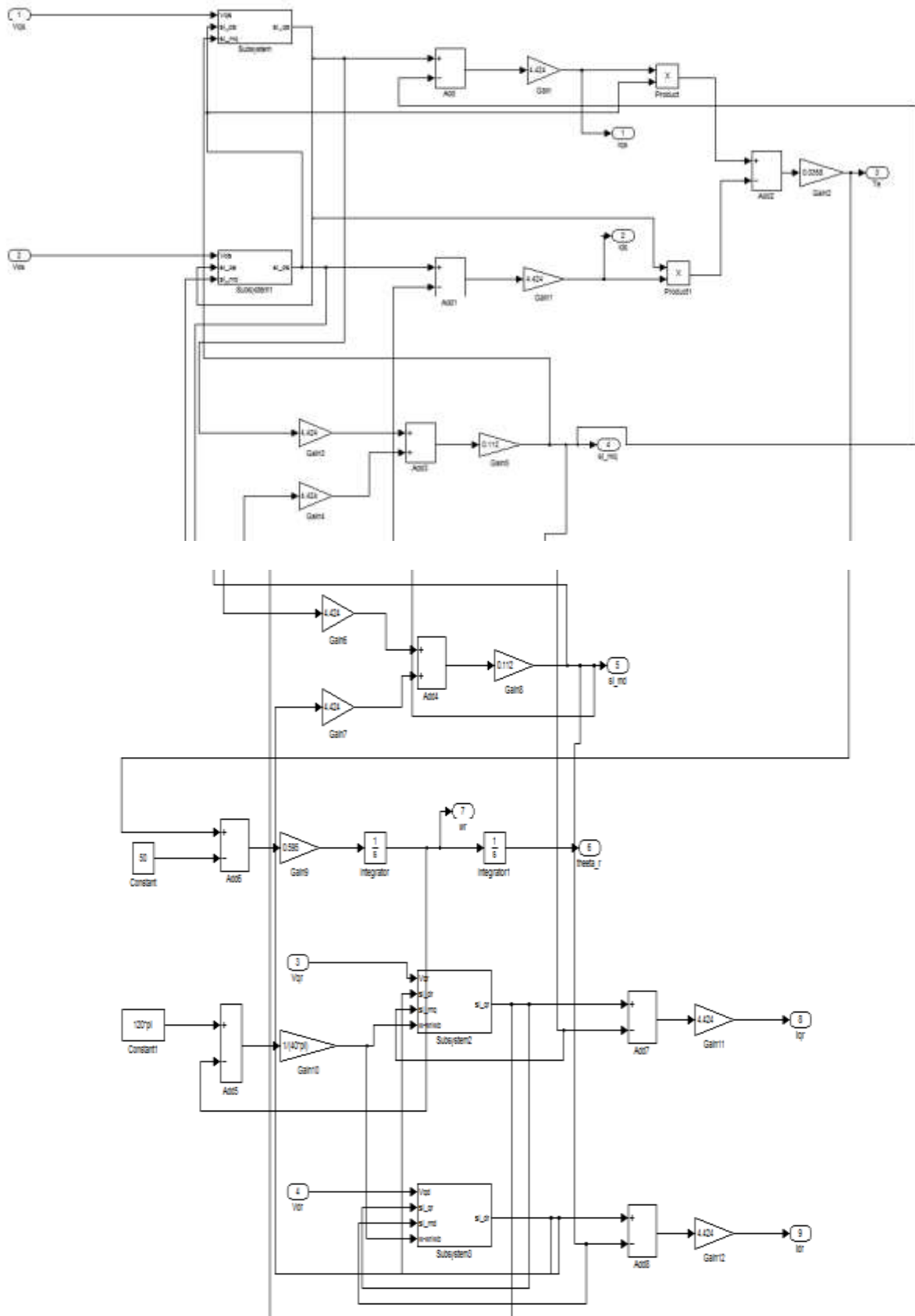


Fig 4.4.2 Simulink Block Diagram for Modelling of DFIG

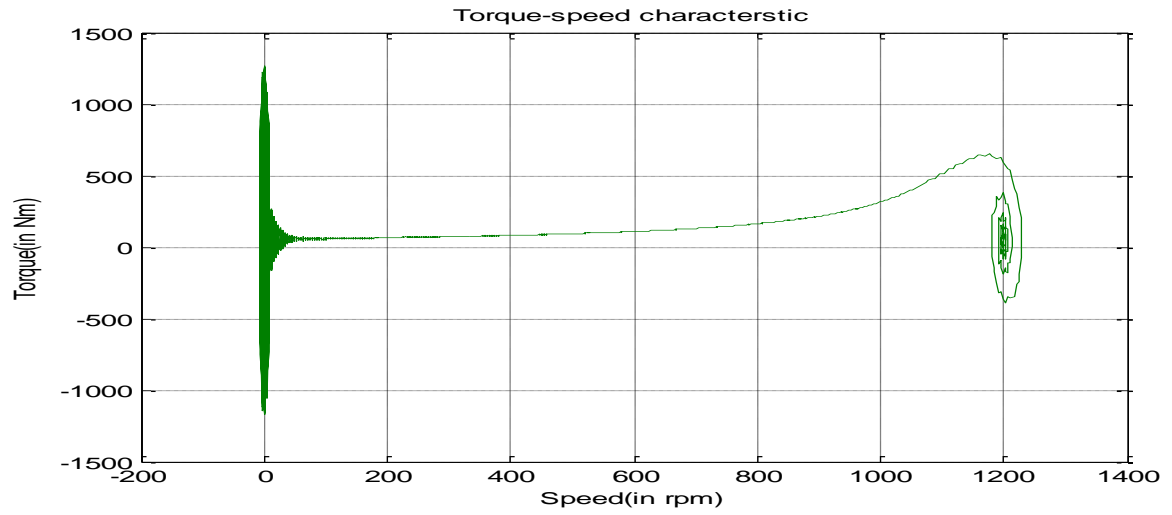


Fig 4.4.3 Torque-speed characteristics

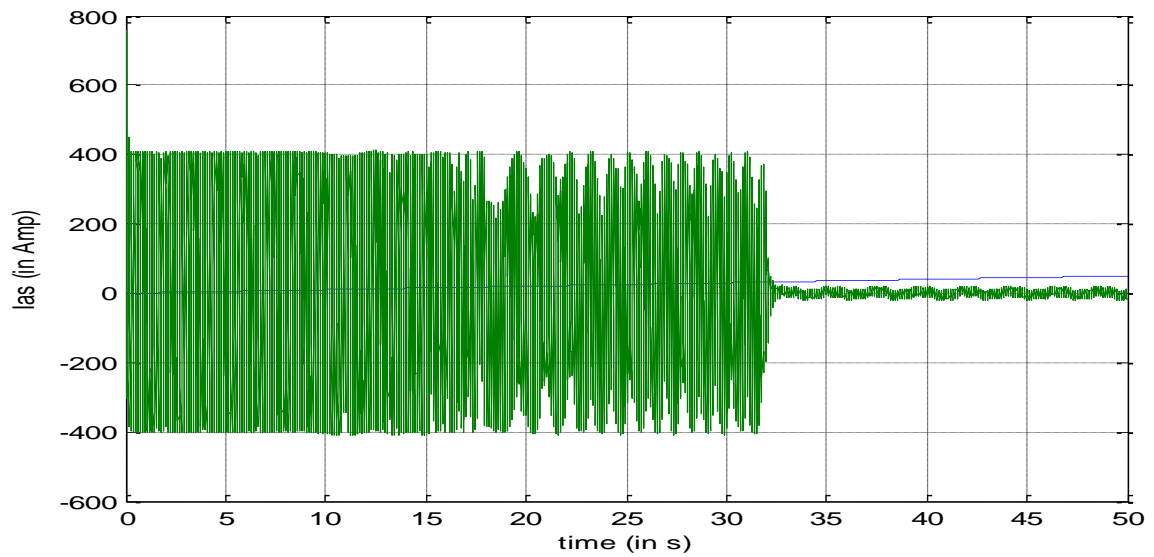


Fig 4.4.4 Stator a-phase current

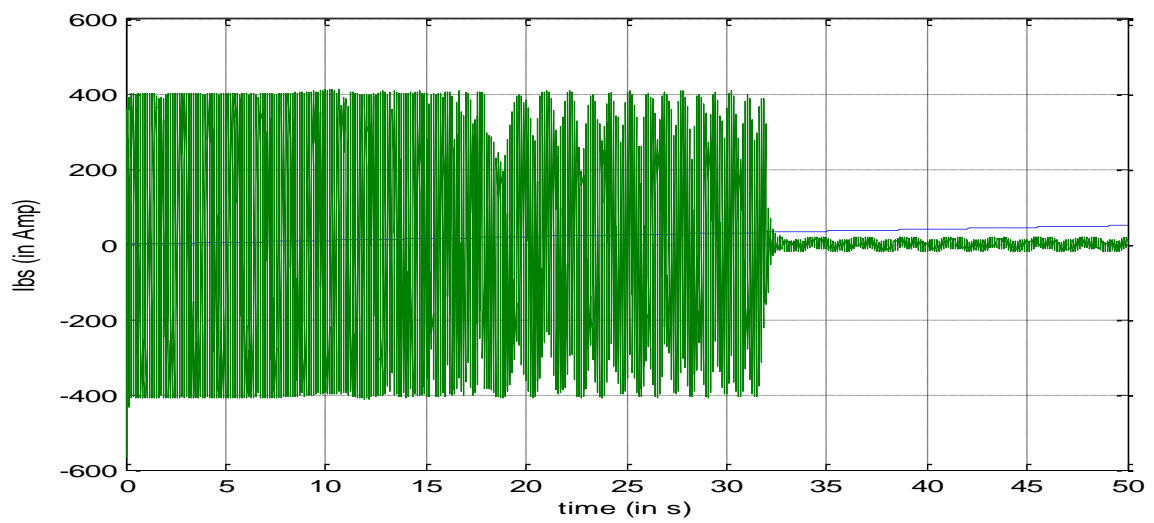


Fig 4.4.5 Stator b-phase current

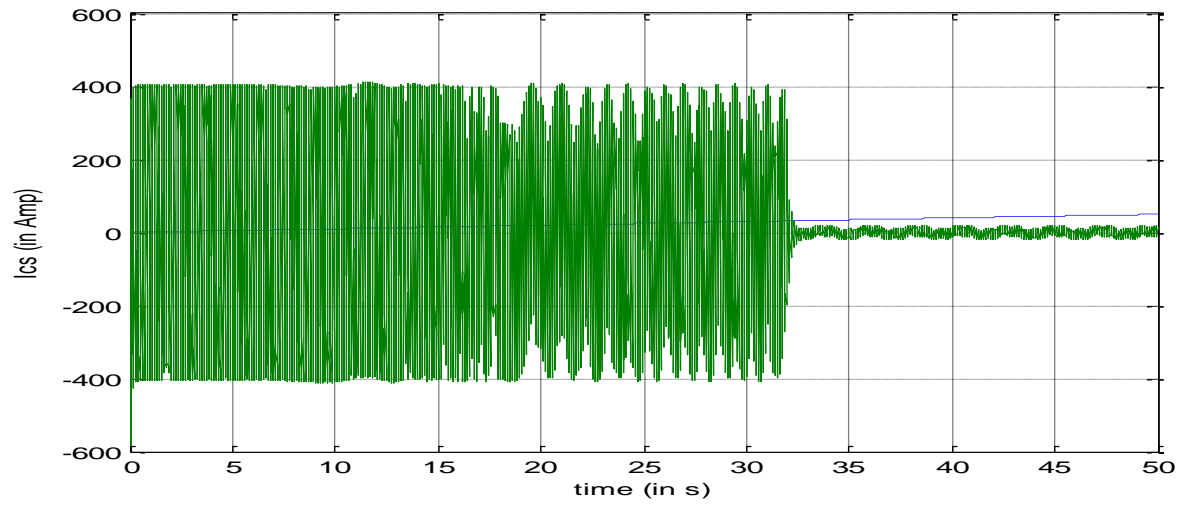


Fig 4.4.6 stator c-phase current

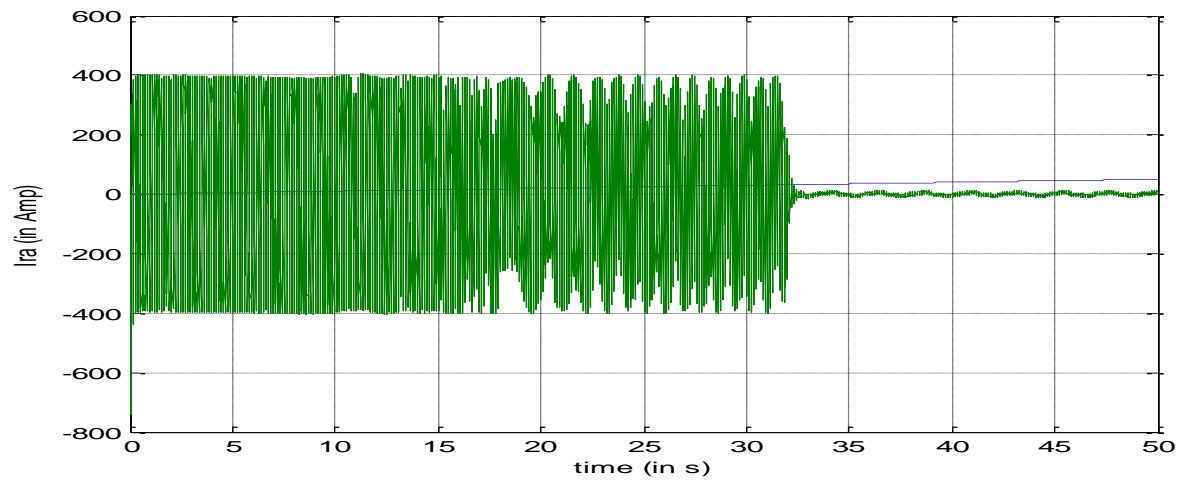


Fig 4.4.7 Rotor a-phase current

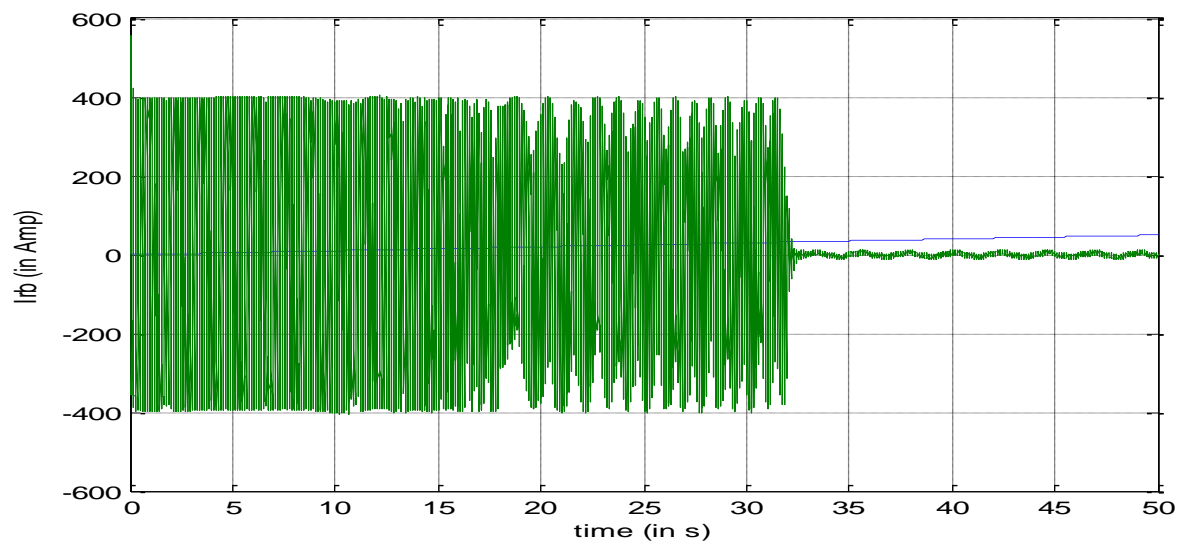


Fig 4.4.8 Rotor b-phase current

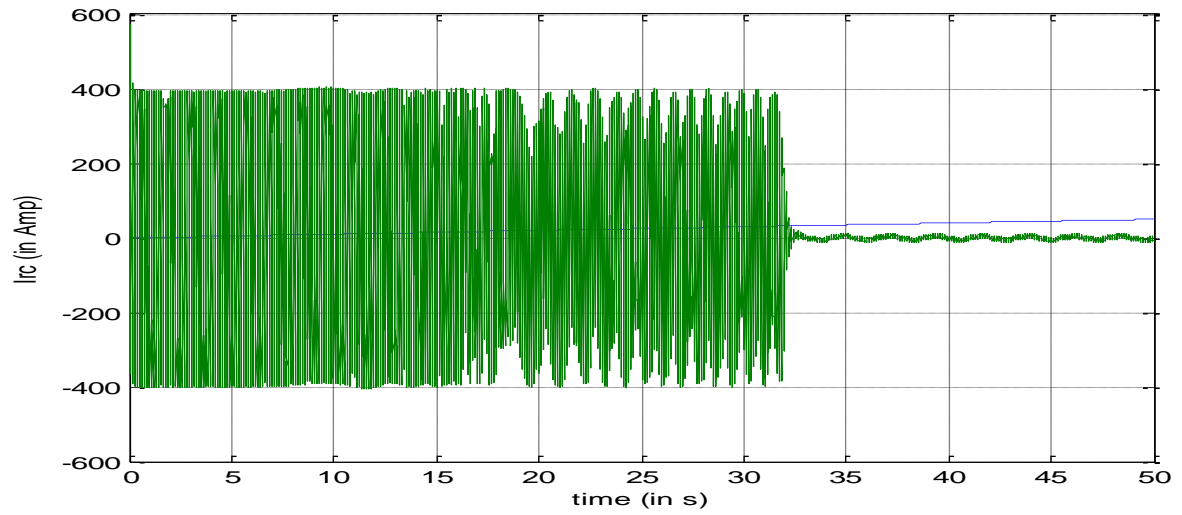


Fig 4.4.9 Rotor c-phase current

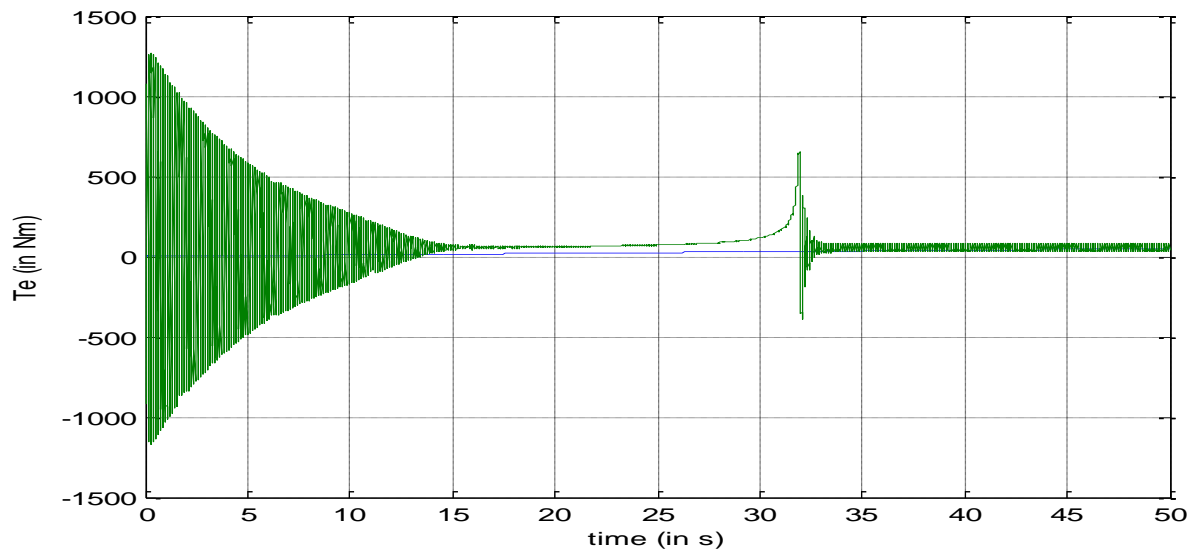


Fig 4.4.10 Electromagnetic torque during free acceleration

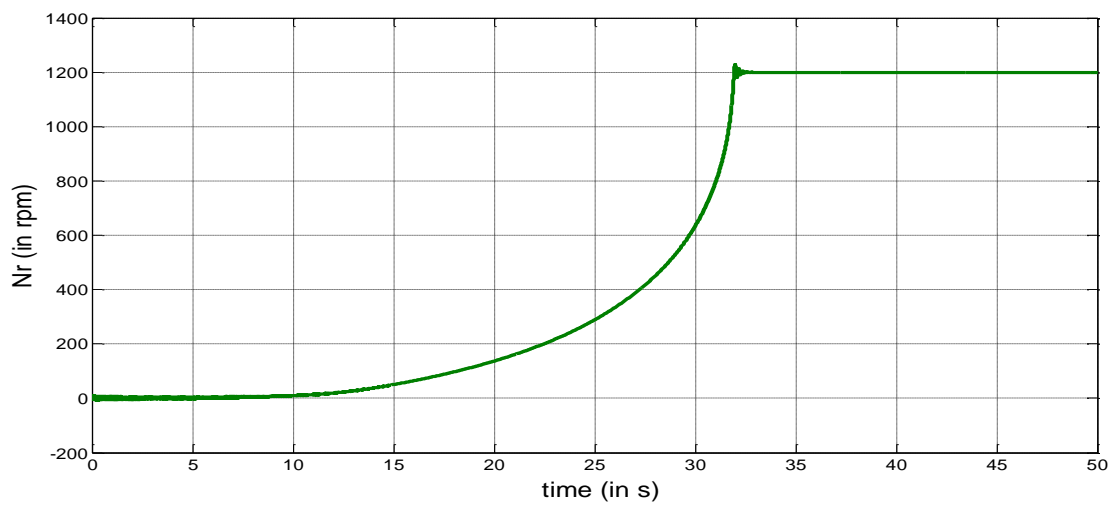


Fig 4.4.11 Rotor speed variation during free acceleration mode

CONCLUSION

The efficiency of DFIG connected wind turbine systems in comparison to other fixed-speed and variable speed wind turbine generator systems are studied . It is found that doubly-fed induction generator wind turbine system's energy efficiency is larger in smaller percentages as compared to other machines. The simulation is carried out by changing the variables from abc to dq0 for simplicity of calculation and simulation. From Plots Power output (P_o) vs wind velocity (V_w) it is observed that maximum power is achieved at optimum value of wind speed beyond this value power is reduced and on increasing the pitch angle the power is also reduced. From plot Power coefficient (C_p) vs Tip speed ratio (TSR) it is observed that on increasing the pitch angle power coefficient is reduced, and plot Toque (T_e) vs Slip (S) characteristics are shows that on increasing the rotor voltage the torque-slip characteristics changes. Modelling of DFIG and Free Acceleration characteristics of induction machine are done using MATLAB/SIMULINK Tool and their outputs are plotted accordingly.

REFERENCE

- [1] S. N. Bhadra, D. Kastha , S. Banerjee, “Wind Electrical Systems ” Oxford University Press 2005
- [2] M. Patel, *Wind and Solar Power Systems: Design, Analysis, and Operation*. Boca Raton, FL: CRC, 2006.
- [3] Rezaei, Esmail, Ahmadreza Tabesh, and Mohammad Ebrahimi. "Dynamic Model and Control of DFIG Wind Energy Systems Based on Power Transfer Matrix", IEEE Transactions on Power Delivery, 2012
- [4] J. Maciejowski, “*Multivariable Feedback Design*,” ser. Electron. Syst. Eng. Ser. Reading , MA: Addison-Wesley, 1989, vol. 1.
- [5] D. Zhi, L. Xu, and B. Williams, “*Model-based predictive direct power control of doubly fed induction generators*,” *IEEE Trans. Power Electron.*,” vol. 25, no. 2, pp. 341–351, Feb. 2010.
- [6] P. Krause, O. Wasynczuk, S. Sudhoff, and I. P. E. Society, “*Analysis of Electric Machinery and Drive Systems*”. Piscataway, NJ: IEEE, 2002
- [7] A. Peterson, “*Analysis, Modeling and Control of Doubly-Fed Induction Generators for Wind Turbines*.” Ph.D. thesis, Chalmers University of Technology, Goteborg, Sweden, 2005.
- [8] D. Zhi, L. Xu, and B. Williams, “*Model-based predictive direct power control of doubly fed induction generators*,” *IEEE Trans. Power Electron.*, vol. 25, no. 2, pp. 341–351, Feb. 2010.
- [9] R. Datta and V. Ranganathan, “*Direct power control of grid-connected wound rotor induction machine without rotor position sensors*,” *IEEE Trans. Power Electron.*, vol. 16, no. 3, pp. 390–399, May 2001.
- [10] J. Hu, H. Nian, H. Xu, and Y. He, “*Dynamic modeling and improved control of DFIG under distorted grid voltage conditions*,” *IEEE Trans. Energy Convers.*, vol. 26, no. 1, pp. 163–175, Mar. 2011.
- [11] S. Muller, M. Deicke, and R. De Doncker, “*Doubly fed induction generator systems for wind turbines*,” *IEEE Ind. Appl. Mag.*, vol. 8, no. 3, pp. 26–33, May/Jun. 2002.
- [12] E. Tremblay, S. Atayde, and A. Chandra, “*Comparative study of control strategies for the doubly fed induction generator in wind energy conversion systems:ADSP-based implementation approach*,” *IEEE Trans. Sustain. Energy*, vol. 2, no. 3, pp. 288–299, Jul. 2011.
- [13] A. Petersson, L. Harnefors, and T. Thiringer, “*Comparision Between Stator-Flux and Grid-Flux-Oriented Rotor Current Control of Doubly-Fed Induction Generators*,” in *Proceedings 35th Power Electronics Specialist Conference*, Vol. 1, Aachen, Germany, 20–25 June 2004, pp. 482–486.
- [14] J. Maciejowski, *Multivariable Feedback Design*, ser. Electron. Syst. Eng. Ser. Reading , MA: Addison-Wesley, 1989, vol. 1.

- [15] R. Krishnan, "*Electric Motor Drives: Modelling, Analysis and Control*," Prentice-Hall of India Private Ltd- 2001.
- [16] J. D. Lavers and R. W. Y. Cheung. 1986. "A software package for the steady state and dynamic simulation of induction motor drives." *IEEE Trans Power Syst.* Vol. PWRS-1, May. pp. 167-173. B. K. Bose. 2007. *Power Electronics and AC Drives*. Pearson Prantice Hall.
- [17] H. Akagi and H. Sato, "Control and performance of a doubly-fed induction machine intended for a flywheel energy storage system," *IEEE Trans. Power Electron.*, vol. 17, no. 1, pp. 109–116, Jan. 2002.
- [18] O. Carlson, J. Hylander, and K. Thorborg, "Survey of variable speed operation of wind turbines," in *Proc. of European Union Wind Energy Conference*, Göteborg, Sweden, May, 20–24, 1996, pp. 406–409.
- [19] N. Hur, J. Jung, and K. Nam, "A fast dynamic dc-link power-balancing scheme for a PWM converter–inverter system," *IEEE Trans. Ind. Electron.*, vol. 48, no. 4, pp. 794–803, Aug. 2001.
- [20] M. Hiller, D. Krug, R. Sommer, and S. Rohner, "A New Highly Modular Medium Voltage Converter Topology for Industrial Drive Applications," in *13th European Conference on Power Electronics and Applications (EPE '09) 2009*, pp. 1–10.
- [21] R. Fadaeinedjad, M. Moallem, and G. Moschopoulos, "Simulation of a wind turbine with doubly fed induction generator by fast and simulink," *IEEE Trans. Energy Convers.*, vol. 23, no. 2, pp. 690–700, Jun. 2008.
- [22] A. Peterson, "Analysis, Modeling and Control of Doubly-Fed Induction Generators for Wind Turbines." Ph.D. thesis, Chalmers University of Technology, Göteborg, Sweden, 2005.
- [23] Lie Xu, "Enhanced Control and Operation of DFIG-Based Wind Farms During Network Disturbances," *IEEE Trans. Energy Conversion*, Vol. 23, No. 4, pp. 1073–1081, December 2008.
- [24] J. B. Ekanayake, L. Holdsworth, X. G. Wu, and N. Jenkins, "Dynamic Modeling of Doubly Fed Induction Generator Wind Turbines," *IEEE Trans. Power Systems*, Vol. 18, No. 2, pp. 803–809, May 2003.

APPENDIX-I

WIND TURBINE GENERATOR'S DATA

PARAMETERS	VALUES	UNITS
Rated Power	1.5	MW
Rated Voltage(Line to Line)	0.545	kV
Rated Frequency	60	Hz
Rated Wind speed	12	m/s
Stator Resistance	1.4	mΩ
Rotor Resistance	0.99	mΩ
Stator Leakage Inductance	89.98	μH
Rotor Leakage Inductance	82.08	μH
Magnetization Inductance	1.526	mH
Stator/Rotor Turns Ratio	1	----
Poles	6	----
Turbine Diameter	8	m
Lumped Inertia Constant	5.04	s